NASA Technical Paper 2423

C.2

May 1985

Calibration of Sonic Valves for the Laminar Flow Control, Leading-Edge Flight Test

Dennis H. Petley,
William Alexander, Jr.,
Andrew S. Wright, Jr.,
and Maria Vallas

NASA

NASA
Technical
Paper
2423

1985

Calibration of Sonic Valves for the Laminar Flow Control, Leading-Edge Flight Test

Dennis H. Petley,
William Alexander, Jr.,
Andrew S. Wright, Jr.,
and Maria Vallas

Langley Research Center
Hampton, Virginia

NASA

National Aeronautics
and Space Administration

Scientific and Technical
Information Branch

Summary

Sonic needle valves were calibrated to measure and control airflow in the suction system for the Leading-Edge Flight Test. This report describes the procedure and results of the calibration flow test. Mass-flow rates and maximum back pressures were measured at total temperatures from −30°F to 75°F and total pressures from 120 to 540 psf over a range of valve settings. Two valves with different nominal sizes were calibrated first, then 41 flight valves were calibrated by comparison with the valve of the same nominal size. Nitrogen was substituted for air, and the method used to convert nitrogen data to air results is discussed. Correlating equations were obtained based on least-squares curve fits of the data. Mass-flow rate was found to be approximately a linear function of total pressure and a square-root function of total temperature. A cubic equation of valve opening length was used to represent the dependence of mass-flow rate on valve opening.

The most important aspect of controlling and measuring mass-flow rate was found to be the setting and measuring of the valve opening length. The valve drive system was found to have significant hysteresis. The setting of the zero reference point was critical to the accuracy of the mass-flow-rate measurement, particularly when measurements were being made with the valve near the closed position. Valve opening length was also found to be dependent on the pressure of the downstream vacuum chamber.

The calibrated flight valves were found to be adequate to measure mass-flow rate over the range of pressures and temperatures expected during the Leading-Edge Flight Test. The correlating equations were used in flight to calculate mass-flow rate.

Introduction

Sonic valves are used in the suction system of the JetStar aircraft at the NASA Dryden Flight Research Facility in the Leading-Edge Flight Test (LEFT). This test, described in reference 1, is part of the Aircraft Energy Efficiency Program (ref. 2) to develop laminar flow technology. The goal of LEFT is to demonstrate the effectiveness and practicality of leading-edge systems in maintaining laminar flow under representative flight conditions. A slotted-surface leading-edge section fabricated by the Lockheed-Georgia Company and a leading-edge section with a perforated titanium porous surface fabricated by Douglas Aircraft Company were installed on the JetStar aircraft for flight testing to determine the effectiveness in obtaining laminar flow. In order to achieve a given chordwise suction profile, it was necessary to control the suction flow into each slot and porous strip. This was accomplished with 41 sonic valves and ducts for 27 slots and 15 porous strips. There are 41 ducts because two of the slots are plumbed together into the same duct. Sonic valves isolate the compressor noise and other noise in the flow downstream of the valve. This isolation of noise may not be needed but is a desirable precautionary measure.

The LEFT suction system consists of ducts routed to sonic valves which are mounted in plenum chambers. Valves of 5/8-inch and 3/4-inch size are used. A 3/4-inch valve is shown in figure 1(a), and typical components of a plenum chamber are shown in figure 1(b). There are three plenum chambers installed in the aircraft cabin, one chamber with 15 sonic valves for the Douglas test article, one chamber with 13 sonic valves for the Lockheed Corporation upper surface, and one chamber with 13 sonic valves for the Lockheed lower surface. A plenum chamber which has been installed in the JetStar aircraft is shown in figure 1(c). After passing through the sonic valves into the chambers, suction air is compressed by a centrifugal turbocompressor and exhausted to the atmosphere.

The sonic valve consists of a fixed nozzle and a movable needle (figs. 1(a) and 1(d)). Although the needle looks more like a plug it is referred to as a needle. The needle position is adjustable to vary the throat area. Downstream of the throat, the nozzle and needle are shaped to provide a divergent section. Air flows into the inlet of the sonic valve at subsonic velocity and moves to the needle where it accelerates to sonic velocity at the throat. Downstream of the throat there is some pressure recovery which results in a higher allowable chamber pressure. Each of the 41 suction lines in LEFT must have a flow controller and a flow meter. To minimize the need for independent flow meters, the sonic valves are calibrated to act as both flow controllers and meters. Operation of the valves at sonic velocity precludes the need for an automatic pressure control system in the chamber because mass flow is independent of downstream pressure when the velocity through the throat is sonic. The aircraft uses an on-board computer to calculate and display mass flow for each sonic valve from measurements of total temperature and total pressure upstream of the throat, needle position, and chamber pressure.

Before flight, it was necessary to calibrate the sonic valves over the expected operating range—total pressures from 120 to 540 psf, mass-flow rates from 0.001 to 0.012 lbm/sec, and total temperatures from −30°F to 75°F. The range of Reynolds number based on length of valve opening from the fully closed position was from 1000 to 40 000. Figure 1(d) shows a 5/8-inch valve with the characteristic dimension x identified. The approach was to first calibrate one valve of each of the two sizes, 5/8 inch and 3/4 inch, then calibrate 41 flight valves by obtaining limited data and comparing with the two calibrated valves. The purpose of this report is to describe the test setup and the results of the calibration flow test of these sonic valves.

Symbols

A_t	throat area
C	discharge coefficient, $\dot{m}_a/\dot{m}_i$
g_c	gravitational constant
K	correlating constant
$\dot{m}$	mass-flow rate
$\dot{m}_a$	measured mass-flow rate
$\dot{m}_c$	corrected mass-flow rate
$\dot{m}_i$	calculated mass-flow rate, isentropic flow being assumed
N	valve number
p	static pressure
p_b	back pressure measured by total-pressure probe
p_c	chamber pressure
p_o	stagnation pressure
p_{ref}	standard pressure, 2116 psf
R	gas constant
Re	Reynolds number
T	static temperature
T_o	stagnation temperature
T_{ref}	standard temperature, 519°R
V	average velocity
x	valve opening length from x_o
x_N	valve opening length for valve N from x_o
x_{cal}	valve opening length for a calibration valve from x_o
x_{out}	output of the displacement transducer, in.
x_o	value of x_{out} when needle is just closed against nozzle
x_J	value of x_{out} when needle is driven closed with predetermined force at operational chamber pressure and chamber temperature
x_{DB}	dead-band difference in x_{out} between just-closed condition and driven-closed condition
Δx_p	change in needle position relative to nozzle caused by change in chamber pressure
Δx_T	change in needle position relative to nozzle caused by change in chamber temperature
γ	ratio of specific heats
ρ	gas density
μ	viscosity
β	$= \frac{x_N - x_{\mathrm{cal}}}{x_{\mathrm{cal}}}$

Description of Test Fixture

The test fixture was an internal flow system into which different chambers and sonic valves could be mounted. The valves are shown in figures 2 and 3, and a schematic diagram of the test fixture is shown in figure 4. The flow system was designed for mass-flow rates from 0.001 to 0.012 lbm/sec, total pressure from 120 to 540 psf, and total temperatures from −30°F to 75°F. The calibration chamber, designed for one sonic needle valve, is shown in figures 4 and 5. This chamber was used to calibrate one 5/8-inch valve and one 3/4-inch valve by interchanging the valves in the flow system. The segment of the flow system from the pressure vessel to the valve entry pipe is shown in figure 6. The gas used in the flow system for the first part of the calibration was dry air. Shortly into the test the gas was changed to dry nitrogen because of the convenience and economy of using a very large tank of dry nitrogen (80 percent of the data were obtained with nitrogen as a test medium). Referring to figure 4, the flow from the compressed gas tanks is controlled with a pressure regulator to set the upstream pressure. A mass-flow meter measures flow rates of warm gas entering the heat exchanger. The heat exchanger consists of copper tubing exposed to cold nitrogen gas boil off from a pool of liquid nitrogen (fig. 7) with a parallel bypass and two valves for controlling the mixing of warm and cold gas. A mass-flow meter for cold gas, the sonic valve and chamber, the vacuum control valve, and piping leading to a 60-foot diameter vacuum sphere are shown in figure 8. The mass-flow-rate data for calibration were obtained from the warm-temperature flow meter. The cold-temperature flow meter was included to test the operation of the flow meter at low temperature.

The calibration data included mass-flow rate, upstream total temperature and total pressure, static pressure just upstream of the throat, needle position relative to the nozzle, and pressure and temperature inside the chamber. Chromel-Alumel (Type K) thermocouples were used for temperature; Datametrics transducers, for pressure; a rotary potentiometer, for displacement; and Hastings meters, for mass-flow measurement. The outputs from the transducers were connected to an electronic signal scanner. The scanner was connected to a microcomputer which was programmed to process, monitor, and print data rapidly. (See fig. 9.) The throat pressure signal was also connected to a digital voltmeter for continuous monitoring to determine when the flow at the throat became subsonic. The maximum chamber pressure for sonic flow at the throat was determined by increasing the chamber pressure from a condition of choked flow until the throat-pressure-voltage output increased approximately 2 percent. The static-pressure tap at the throat was located in the needle part of each of the two calibration valves. The hole diameter of these pressure taps was 0.02 inch (0.04-inch-diameter holes were found unacceptable and were redrilled slightly upstream with the 0.02-inch diameter). The location of the pressure tap in the needle for the 5/8-inch and 3/4-inch calibration valves is shown in figure 10.

The position of the needle relative to the nozzle is set by operating the worm-gear-drive motor. The needle is mounted on the end of an aluminum-alloy shaft which has a worm gear drive on the opposite end to drive the valve toward the open or closed direction, depending on direction of rotation of the electric motor. A rotary potentiometer was used to indicate the position of the needle. (See fig. 5.) The reference point for the needle position relative to the nozzle was found by driving the needle into the nozzle with a small force. The maximum hysteresis was 0.05 inch. When an outward adjustment in needle position was made, an inward adjustment greater than or equal to 0.05 inch of change in the needle position was required to insure that all the hysteresis had been taken out. Another method, which was used to insure that the hysteresis was taken out, was to move the needle inward until both the mass-flow rate and needle position readings decrease while the upstream and downstream pressures were maintained approximately constant. All the valves tested, which included single calibration valves mounted in the calibration chamber (fig. 5) and multiple valves mounted in the flight chamber (fig. 11), operated in the same way. The throat pressure measurement was made only when a calibration valve was mounted in the calibration chamber.

Calibration Procedure

Valves with nominal sizes of 5/8 inch (fig. 2) and 3/4 inch (fig. 3) were calibrated over a range of temperatures, pressures, and mass-flow rates. The approach was to obtain a complete calibration for one valve of each of the two sizes, referred to as calibration valves, then calibrate flight valves by taking a minimum amount of data and comparing each valve with the calibration valve of the same nominal size.

A mass-flow-rate calibration and a choke pressure calibration were obtained for each of the two calibration valves, whereas only a mass-flow-rate calibration was obtained for each of the flight valves. For a mass-flow-rate calibration data point, the required information was mass-flow rate as a function of upstream total temperature, upstream total pressure, and the needle position relative to the nozzle, or

$$\dot{m} = f(T_o, p_o, x)$$

The distance x can be used here because throat area is a function of x. For this part of the calibration, the valve back pressure was maintained low enough to insure choked flow. For a choke pressure data point, the required information was chamber pressure as a function of the same measurements, that is,

$$p_c = g(T_o, p_o, x)$$

To obtain this data point, the chamber pressure or back pressure is initially set low enough to insure choked flow. The chamber pressure is then increased until the flow becomes subsonic at the throat, which is indicated by a decrease in mass-flow rate and/or a 2-percent increase in the pressure. The choke pressure data point is then recorded.

The procedure is given for sonic calibration of a typical valve. Either a calibration chamber and valve or a flight chamber with one connected valve and all others plugged was installed in the flow system. The vacuum sphere pressure was decreased enough to produce choked flow at the desired total pressure. The vacuum sphere valve was set to the full-open position. For total temperatures other than room temperature, liquid nitrogen was added to the heat exchanger box. The sonic valve was opened enough to obtain a flow rate of 0.01 lbm/sec or more, and the pressure regulator and heat exchanger valves were adjusted to obtain the desired total pressure and total temperature. These conditions were maintained until the temperatures stabilized (very little time was needed when testing at room temperature). With the temperature stabilized, the valve needle was adjusted inward to the desired x setting. The pressure regulator and heat exchanger valves were adjusted as needed to obtain the desired total pressure and total temperature, and the microcomputer command to record data was initiated. If choke pressure limit data were desired for a calibration valve, they were obtained at this time (flight valves do not have throat pressure taps and choke pressure data were not obtained for these valves). To obtain choke pressure data, the vacuum sphere valve was gradually adjusted toward the closed position until the throat pressure increased by approximately 2 percent with the total pressure and total temperature held constant, and the command to record data was again initiated. The procedure was repeated for other total-pressure settings with the x setting and T_o setting maintained constant until an entire set of data were obtained for this x setting and T_o setting. The x setting was then changed to another desired x data value and the procedure was repeated. All data were obtained for a T_o setting before a change to another T_o setting.

Results for Calibration Valves

Both the mass-flow-rate calibration and the choke pressure calibration were done on each of the calibration valves. The temperature range from room temperature to −30°F was covered by taking data at three different nominal temperatures, 75°F (room temperature), 10°F, and −30°F. Nitrogen gas was used for most of the 10°F and −30°F data and a small correction was applied to derive the data for air (the air data are given in the appendix). The mass-flow-rate data for the 5/8-inch and 3/4-inch calibration valves are plotted in figures 12 and 13. Most of the data were obtained at temperatures near the nominal temperature. The actual range of measurements for each of the three nominal temperatures were 70°F to 80°F for the nominal 75°F, −15°F to 21°F for the nominal 10°F, and −55°F to −17°F for the nominal −30°F. The maximum expected errors in mass-flow rate caused by temperature variation from nominal temperature are 0.5 percent for the 75°F data, 2 percent for the 10°F data, and 3 percent for the −30°F data (based on the square root of the absolute temperature dependence). The choke pressure calibration data are plotted in figures 14 and 15. The conversion from nitrogen data to air data was made by using data for actual mass-flow rate divided by isentropic mass-flow rate per unit area at the throat versus Reynolds number (fig. 16), and chamber pressure divided by total pressure versus Reynolds number (fig. 17). The characteristic dimension in the Reynolds number was the length of valve opening. (See fig. 1(d).) Figures 16 and 17 were obtained from measured data for the valve opening length x, total pressure p_o, total temperature T_o, measured mass-flow rate $\dot{m}_a$, and chamber pressure p_c by using the following isentropic ideal gas relationships at a Mach number of 1:

$$p = (0.5283)p_o$$

$$T = (0.8333)T_o$$

$$V = (\gamma R T g_c)^{1/2}$$

$$\rho = \frac{p}{RT}$$

$$\mathrm{Re} = \frac{\rho V x}{\mu}$$

$$\dot{m}_i = \rho V A_t$$

$$\frac{\dot{m}_i}{A_t} = \rho V$$

where R is 55.16 ft-lbf/lbm-°F for nitrogen and 53.3 ft-lbf/lbm-°F for air. The vertical axis of figure 16 is defined by the following equations:

$$\frac{A_t \dot{m}_a}{\dot{m}_i} = \frac{\dot{m}_a}{\dot{m}_i/A_t} = \frac{\dot{m}_a}{\rho V}$$

and viscosity μ values were obtained from table 1. Air data were derived from nitrogen data by making adjustments of measured mass-flow rate $\dot{m}_a$ and chamber pressure p_c. Using figures 16 and 17, adjusted values of $\dot{m}_a$ and p_c for air were obtained from Reynolds number and isentropic mass-flow rate per unit area based on measured T_o, measured p_o, R for air, and μ for air. The expressions for air-adjusted $\dot{m}_a$ and p_c were:

$$(\dot{m}_a)_{\mathrm{air}} = \left(\frac{A_t \dot{m}_a}{\dot{m}_i}\right)_{\mathrm{nit}} \left(\frac{\dot{m}_i}{A_t}\right)_{\mathrm{air}}$$

$$(p_c)_{\mathrm{air}} = \left(\frac{p_c}{p_o}\right)_{\mathrm{nit}} (p_o)_{\mathrm{air}}$$

A correlation of the cold-temperature mass-flow data was needed so that the data could be used more easily during flight. A plot of corrected mass flow versus needle position for the cold-temperature data indicated that these parameters could be used to correlate the data. The corrected mass-flow rate is

$$\dot{m}_c = \dot{m}_a \left(\frac{p_{\mathrm{ref}}}{p_o}\right) \left(\frac{T_o}{T_{\mathrm{ref}}}\right)^{1/2}$$

where T_{ref} is 519°R, and p_{ref} is 2116 psf. Least-squares curve fits of the calibration valve data for corrected mass-flow rates are shown in figures 18 through 21. The equations for the least-squares curve fits are given as follows:

For the 5/8-inch valve at low temperature (nominal stagnation temperatures of 10°F and −30°F),

$$\dot{m}_c = -0.012217 + 5.4419x + 5.688x^2 - 4.7108x^3$$

and for the 3/4-inch valve at low temperature,

$$\dot{m}_c = -0.003505 + 5.6292x + 9.9917x^2 - 9.07983x^3$$

For the 5/8-inch valve at room temperature (nominal stagnation temperature of 75°F),

$$\dot{m}_c = -0.017289 + 6.7134x - 0.59361x^2 + 3.9667x^3$$

and for the 3/4-inch valve at room temperature,

$$\dot{m}_c = -0.004664 + 7.1942x + 3.6826x^2 - 2.4683x^3$$

where the units for $\dot{m}_c$ and x are lbm/min and inches, respectively.

Suction Flow for Flight Valves

There are three chambers and a total of 41 flight valves which were calibrated. The chambers are numbered 1, 3, and 5 (the chambers numbered 2 and 4 were deleted from the program). Chamber 1 has 15 valves for the Douglas test article, chamber 3 has 13 valves for the Lockheed upper surface test article, and chamber 5 has 13 valves for the Lockheed lower surface test article. The chambers are designed to accommodate up to 15 valves and the valve mounting ports are numbered 1 to 15. The flight valves are identified by the chamber number and mounting port number. The four valve numbers which were not used are chamber 3, valves 1 and 7 and chamber 5, valves 13 and 14. The calibration of the flight valves was accomplished by a position calibration of each flight valve for the same flow conditions as the calibrated valve. This section describes how the results of the 5/8-inch calibrated valve were applied to the flight valves.

Each flight valve of a chamber assembly had a valve position versus voltage output calibration curve. The flow line was attached to the valve to be tested and the other valves were plugged. At four or five different valve settings, the mass-flow rate, the total pressure, and the total temperature were recorded. The value of x_{cal} was determined at each flow condition for measured p_o, T_o, and $\dot{m}$ based on the calibration-valve map. Ideally, x_N and x_{cal} would be equal for the same p_o, T_o, and $\dot{m}$. (See fig. 1(d).) Because of manufacturing tolerances and other differences between valves, x_N and x_{cal} were not equal. The data to correlate each flight valve to the same size calibrated valve are shown in figures 22, 23, and 24. These figures give the calibration parameter β versus valve position x_N, where β is defined as

$$\beta = \frac{x_N - x_{\text{cal}}}{x_{\text{cal}}}$$

Over a small range of x, the mass-flow rate is nearly a linear function of x so that $\beta \times 100$ is the percent difference between the mass flow of valve N and the mass flow of the calibration valve for the same p_o, T_o, and x setting. The plot of β versus x_N calibrates each flight valve by comparison with the same size calibration valve.

Before and after each test, the valve was closed to check the x_o positions with the chamber at atmospheric conditions and with the chamber at operational pressure and temperature. The x_o values for flight valves are given in table 2. The Δx_p factor given is the amount the valve attachment plate deflected when the chamber pressure was lowered to approximately 100 psfa. (See fig. 11.) This factor should be included when the actual valve position x_N is determined because a different chamber pressure would produce a different plate deflection. The x_o value should be adjusted by an amount Δx_p which is approximately a linear function of Δp.

Purge Flow Correlation for Flight Valve

One requirement of the flow system is to provide a controlled purge flow (flow in the opposite direction from the suction case previously discussed) to keep the suction system free from contamination when the aircraft is at low altitude. The valve operates from subsonic to sonic speeds at the throat when the flow is in the purge direction. Less accuracy is needed for this correlation so an approximate correlation was obtained for one representative 5/8-inch valve. The correlation is accurate within ±6 percent mass-flow rate for x settings from 0.02 to 0.10 inch, for chamber pressures (upstream pressures) from 2000 to 4400 psf and for pressure ratios (pressure measured by rearward-facing total-pressure probe divided by chamber pressure, fig. 1(d)) less than 0.7. Errors in measurement of x could cause mass-flow-rate errors greater than ±6 percent. The correlating equation which is applicable for subsonic or sonic flow is

$$\dot{m} = \frac{Kp_c}{\sqrt{T_o}}\left(\frac{p_c}{p_b}\right)^{0.1} \qquad \left(\frac{p_b}{p_c} < 0.7\right)$$

where

$$K = \frac{105.45x - 1.099}{10^5}$$

and p_b is back pressure, measured by the rearward-facing total-pressure probe, and the units for K are lbm/sec($\sqrt{°R}$/psf); for x, inches; for p_c and p_b, psf; for T_o, °R; and for $\dot{m}$, lbm/sec. If the flow is sonic at the throat, the pressure ratio p_b/p_c which would occur at the sonic condition should be used in the mass-flow-rate equation. The best data fit is shown in figure 25. The minimum back pressure for subsonic flow must be determined from figure 26, based on p_c and x.

Discussion of Valve Characteristics

In the process of performing the flow calibration, several observations were made dealing with the valve design and performance. The purpose of the valve is to control and measure mass-flow rate accurately with sonic flow at the throat and a minimum of total-pressure loss. Minimizing pressure loss is equivalent to maximizing pressure recovery p_c/p_o, which allows sonic flow to be achieved with higher chamber pressures. The correlation for corrected mass-flow rate as a function of x (figs. 18 to 21) can be used to set the mass-flow rate, and the plots of pressure ratio versus total pressure (figs. 14 and 15) can be used to insure that the flow is sonic. Greater mass-flow-rate accuracy can be obtained by using the data of $\dot{m}$ versus p_o for the closest temperature after obtaining x_{cal} from x_N by using the plot of $(x_N - x_{\text{cal}})/x_{\text{cal}}$ versus x_N for the particular valve. A temperature correction can be made by multiplying $\dot{m}$ thus obtained by the square root of the absolute temperature ratio.

The needle position control was found to be important in setting and measuring mass flow. The mass-flow rate depends on the x position of the needle as well as the amount of misalignment between the centerline of the needle and the centerline of the nozzle. Based on the characteristics of flow through an eccentric annulus, centerline misalignment should produce higher mass-flow rates for the same x position and p_o (ref. 3). Errors in the position of the needle become most critical when the valve is near the closed position. The following equations were used to obtain the position of the needle relative to the closed position for valve N, that is x_N:

$$x_N = x_{\text{out}} - x_o$$

where x_{out} is the output of the displacement transducer in inches, and x_o is x_{out} when the needle is just closed against the nozzle;

$$x_o = x_J + x_{DB}$$

where x_J is x_{out} when the needle is driven closed with a predetermined force at the operational chamber pressure and chamber temperature, and x_{DB} is the difference in x_{out} between the just-closed condition and driven-closed condition $(x_o - x_J)$. The magnitude of x_{DB} was minimized by closing the needle with a small force. The x_{DB} value was different for each valve and drive system combination. More direct x measurements could have been made if a linear voltage displacement transducer had been mounted near the needle. The x_J value depends on chamber pressure and chamber temperature. A change in chamber pressure causes a change in the loading and resulting deflection of the flat end plates and thus changes the position of the needle and nozzle. A change in chamber temperature causes a change in length and perhaps an angular deflection of the needle support shaft. If x_J is obtained at one set of chamber conditions but is to be used at another, adjustments should be made as follows:

$$x_J = x_{J,\text{ref}} + \Delta x_p + \Delta x_T$$

where $x_{J,\text{ref}}$ is the value of x_J at reference chamber conditions, Δx_p is the change in needle position relative to nozzle when chamber pressure changes, and Δx_T is the change in needle position relative to nozzle when shaft temperature changes. Figure 27 shows that the area of the throat is approximately a linear function of x and, therefore, the mass-flow rate is sensitive to the x position. The calibration of a flight valve was repeated to test the accuracy of the x setting and resulting mass-flow rate. The results of the original calibration and recalibration of valve 6 of chamber 5 are shown in figure 28. The two calibrations of this valve are in excellent agreement for x_N greater than 0.1 inch. The difference between the data points at $x_N = 0.08$ inch indicates that a 2-percent error in x setting for a given p_o, T_o, and $\dot{m}$ (or a 2-percent error in $\dot{m}$ for a given p_o, T_o, and x setting) can be expected for x_N less than 0.1 inch.

The valve characteristics considered important for high pressure recovery were x setting, length and rate of contraction and expansion, and smoothness of internal surfaces. When the valves were operated toward the open position, recovery was high and it was low for x settings less than about 0.1 inch. The length of contraction can be much shorter than expansion but the length appeared extremely short in this design. Increasing the contraction length should increase the pressure recovery. The performance of the contraction segment of the valve can be represented by plots of discharge coefficient versus Reynolds number. (See figs. 29 and 30.) The discharge coefficient for a sonic nozzle is defined by the following equation:

$$C = \frac{\dot{m}_a}{\dot{m}_i}$$

For fixed-geometry sonic nozzles, discharge coefficients of about 0.97 are usually observed (ref. 4). The measured discharge coefficients were from 0.69 to 0.975 for the 5/8-inch valve and from 0.70 to 0.97 for the 3/4-inch valve. When the valve is nearly closed, the rate of expansion is such that separation and resulting high pressure losses are expected. When the valve is near the full-open position, more expansion length would be beneficial. However, in the present application, the valve is operated more toward the closed position. The smoothness of internal surfaces is important to minimize skin friction and prevent flow separation. Pressure recovery can be increased by smoothing the cone cylinder intersections in the nozzle, particularly the one near the throat which is subjected to high-speed flow.

If the boundary layer at the throat is thin, the chamber pressure would not be expected to effect the mass-flow-rate measurement. A thick subsonic boundary layer will allow downstream pressure disturbances to pass upstream and, thus, the mass-flow rate would be affected by chamber pressure. The rate of contraction in these valves precludes significant boundary-layer development. The boundary-layer effect must be small because the plots of mass-flow rate versus total pressure are linear for constant x even though the chamber pressure varied in a random manner.

Concluding Remarks

The sonic valves for the Leading-Edge Flight Test were successfully calibrated for control and measurement of suction mass-flow rates from 0.001 to 0.012 lbm/sec for total pressures from 120 to 540 psf and total temperatures from −30°F to 75°F. Two valves, one of 5/8-inch nominal size and the other of 3/4-inch nominal size, were calibrated first. The 41 flight valves consisting of duplicate valves of one of the two sizes were then calibrated by comparison to the first two valves. The calibration was repeatable. A correlating equation was obtained from mass-flow rate as a function of total pressure, total temperature, and valve setting. Required pressure ratios for sonic flow were measured over the specified range of total pressure, total temperature, and mass-flow rate. The range of measured discharge coefficients was from 0.69 to 0.975 for the 5/8-inch valve and from 0.70 to 0.97 for the 3/4-inch valve, compared with a value of about 0.97 usually observed for fixed-geometry sonic nozzles.

The most critical part of measuring the mass-flow rate through this variable-throat-area valve is measurement of valve opening length x, and mass-flow-rate sensitivity to x is greatest for small x. A significant part of the x measurement is the determination of the zero point, the x value when the valve is just closed and the flow rate is approximately zero. The measurements of x were sufficient to obtain the required mass-flow-rate accuracy. Less sensitivity to x and therefore improved accuracy could be obtained by using smaller similarly designed valves.

The pressure recovery of the valves was generally good. The range of required pressure ratios for sonic flow was from 0.57 to 0.83 for the 5/8-inch valve and from 0.53 to 0.82 for the 3/4-inch valve. When the valves were operated toward the open position, the recovery of pressure was highest; in other words, the highest chamber pressures can be used. Conversely, when the valves were operated toward the closed position, x less than about 0.1 inch, the recovery of pressure was considered low; in other words, low chamber pressures were needed. Smaller valves would operate more toward the open position; therefore, pressure recovery could have been improved by using smaller similarly designed valves.

Although some areas of possible valve improvement have been mentioned, the calibrated flight valves are considered adequate to control and measure mass-flow rate over the range of pressures and temperatures expected during the Leading-Edge Flight Test of the Laminar Flow Program. The low temperature correlating equations for the 5/8- and 3/4-inch calibration valves were used in flight to calculate mass-flow rate from flight measurements of total pressure, needle position, and chamber pressure and temperature. After completion of flight tests, more accurate calculations of mass-flow rate can be made as needed by using calibration data as described herein.

NASA Langley Research Center
Hampton, VA 23665
February 19, 1985

Appendix

Air Data for 5/8-Inch and 3/4-Inch Calibration Valves

The air adjusted data for the 5/8-inch and the 3/4-inch calibration valves are included in this appendix. Data at three different nominal temperatures are given for each of the two valves. The required chamber pressure to produce sonic flow was entered into the chamber pressure column. When the chamber pressure was below the pressure required for choked flow, a flag value of −1.0 was entered in the chamber pressure column.

TEST DATA FOR 5/8-INCH VALVE AT -30°F

Temperature, °F	Mass-flow rate, (lbm/sec)*100	Total pressure, psf	Chamber pressure, psf	Valve opening length, in.
-33.400	.10792	555.110	-1.00000	.0420
-24.970	.20991	538.370	-1.00000	.0805
-30.140	.10392	306.200	-1.00000	.0805
-25.280	.30964	531.460	-1.00000	.1133
-23.980	.31087	585.150	363.28742	.1133
-23.020	.21136	354.590	-1.00000	.1133
-20.920	.22721	412.390	240.09520	.1133
-17.440	.10315	191.330	-1.00000	.1133
-31.270	.41843	537.210	-1.00000	.1432
-29.290	.42337	552.230	413.57480	.1432
-24.610	.31405	424.760	-1.00000	.1432
-21.910	.31629	440.070	322.48157	.1432
-31.450	.21744	304.710	-1.00000	.1432
-27.080	.21458	303.910	211.53894	.1432
-22.420	.11252	165.730	-1.00000	.1432
-42.580	.61788	532.690	-1.00000	.2007
-41.140	.62024	537.590	431.23676	.2007
-36.940	.39916	369.550	-1.00000	.2007
-34.600	.40574	379.180	284.50526	.2007
-28.480	.20900	205.510	-1.00000	.2007
-24.380	.21426	215.950	144.72720	.2007
-34.360	.82126	542.060	-1.00000	.2606
-32.750	.82157	547.880	457.01604	.2606
-29.470	.62719	414.310	-1.00000	.2606
-27.350	.62154	411.280	332.88048	.2606
-21.820	.41841	278.850	-1.00000	.2606
-19.430	.43669	294.360	227.95240	.2606
-48.050	.81629	421.470	-1.00000	.3211
-47.020	.81722	428.830	355.36257	.3211
-44.540	.62471	322.370	-1.00000	.3211
-42.560	.62274	322.210	266.08774	.3211
-41.140	.41473	217.620	-1.00000	.3211
-29.960	.26234	140.910	-1.00000	.3211
-26.770	.26855	150.960	110.76636	.3211
-38.470	.83691	365.200	-1.00000	.3789
-36.170	.84157	368.180	305.40672	.3789
-31.990	.62293	274.540	-1.00000	.3789
-30.280	.63520	285.260	226.95081	.3789
-25.100	.41972	190.310	-1.00000	.3789
-22.360	.42888	195.380	150.83266	.3789
-21.230	.34866	152.800	-1.00000	.3789
-20.110	.35324	165.890	129.44813	.3789

Temperature, °F	Mass-flow rate, (lbm/sec)*100	Total pressure, psf	Chamber pressure, psf	Valve opening length, in.
-44.500	.84208	310.480	-1.00000	.4381
-44.500	.84689	311.840	257.34394	.4381
-42.400	.62228	234.980	-1.00000	.4381
-41.320	.63722	244.810	192.75536	.4381
-35.320	.41339	156.960	-1.00000	.4381
-33.280	.42007	163.370	127.06040	.4381
-42.880	.81533	267.620	-1.00000	.4976
-41.800	.81235	270.350	217.88923	.4976
-38.420	.62860	205.540	-1.00000	.4976
-36.980	.62770	205.650	163.06513	.4976
-30.050	.40462	137.010	-1.00000	.4976
-27.580	.41159	139.680	105.79032	.4976

TEST DATA FOR 5/8-INCH VALVE AT 10°F

Temperature, °F	Mass-flow rate, (lbm/sec)*100	Total pressure, psf	Chamber pressure, psf	Valve opening length, in.
.080	.11061	550.660	-1.00000	.0444
11.350	.21005	545.590	-1.00000	.0814
13.340	.21022	552.890	315.01000	.0814
15.620	.10380	292.010	-1.00000	.0814
2.660	.31860	540.160	-1.00000	.1178
5.090	.32184	547.850	359.33047	.1178
7.700	.21203	368.280	-1.00000	.1178
9.820	.21280	370.450	243.38635	.1178
11.980	.10648	194.990	-1.00000	.1178
4.010	.41054	523.430	-1.00000	.1513
6.170	.40790	530.730	396.08132	.1513
8.690	.31939	419.240	-1.00000	.1513
10.220	.31821	417.960	296.97934	.1513
13.340	.20944	280.870	-1.00000	.1513
15.350	.21700	291.150	204.90427	.1513
20.800	.10873	141.080	-1.00000	.1513
2.800	.51532	536.480	-1.00000	.1780
3.470	.51999	543.350	423.79876	.1780
7.430	.30537	336.130	-1.00000	.1780
9.190	.31340	345.490	249.58076	.1780
13.880	.21341	239.220	-1.00000	.1780
15.170	.21482	241.340	172.10695	.1780
16.210	.10897	127.510	-1.00000	.1780
-4.660	.62251	546.090	-1.00000	.2050
-3.640	.62750	553.580	439.59027	.2050
-.580	.42329	375.980	-1.00000	.2050
1.340	.42570	378.890	289.58681	.2050
6.130	.20643	196.690	-1.00000	.2050
9.230	.20777	198.620	144.99249	.2050
13.400	.16239	152.730	-1.00000	.2050
-1.430	.81705	539.220	-1.00000	.2720
-.100	.81750	542.040	448.55493	.2720
3.560	.63086	410.520	-1.00000	.2720
6.260	.63657	415.450	332.74843	.2720
9.590	.41953	275.640	-1.00000	.2720
11.750	.42244	278.180	213.01826	.2720
15.940	.21611	149.090	-1.00000	.2720
18.950	.21680	151.820	109.71251	.2720
-7.240	.83566	426.350	-1.00000	.3372
-6.570	.84002	430.450	356.43063	.3372
1.810	.61190	310.390	-1.00000	.3372
2.930	.61022	309.870	253.57908	.3372

Temperature, °F	Mass-flow rate, (lbm/sec)*100	Total pressure, psf	Chamber pressure, psf	Valve opening length, in.
5.990	.41551	215.670	-1.00000	.3372
10.130	.27718	147.970	-1.00000	.3372
11.480	.27804	148.640	109.08642	.3372
-10.890	.82562	344.570	-1.00000	.4020
-9.450	.82387	343.340	277.68767	.4020
-7.740	.62174	258.520	-1.00000	.4020
-3.550	.62211	259.880	207.99262	.4020
-1.160	.42362	177.810	-1.00000	.4020
1.450	.42865	180.320	139.63987	.4020
4.190	.31597	137.220	-1.00000	.4020
5.230	.31651	139.280	104.06459	.4020
.800	.81087	296.250	-1.00000	.4713
1.990	.80960	297.780	241.57383	.4713
5.500	.62848	223.350	-1.00000	.4713
7.300	.63603	228.060	181.93576	.4713
11.080	.41840	149.810	-1.00000	.4713
13.040	.42008	151.810	116.45482	.4713
6.940	.82840	262.090	-1.00000	.5384
6.890	.83053	264.090	213.78950	.5384
9.140	.61668	190.910	-1.00000	.5384
9.820	.62123	193.690	150.72191	.5384
12.500	.41417	129.340	-1.00000	.5384
14.590	.41729	131.400	96.49296	.5384

TEST DATA FOR 5/8-INCH VALVE AT 75^{o}F

Temperature, ^{o}F	Mass-flow rate, (lbm/sec)*100	Total pressure, psf	Chamber pressure, psf	Valve opening length, in.
72.140	.10160	542.330	-1.00000	.0438
72.770	.09630	526.730	309.85000	.0438
73.270	.20660	534.460	-1.00000	.0772
69.800	.20750	538.890	361.77000	.0772
73.630	.15670	413.090	-1.00000	.0772
73.760	.15620	414.730	272.50000	.0772
73.720	.10900	296.140	-1.00000	.0772
73.850	.10830	298.870	182.68000	.0772
74.080	.29870	552.420	-1.00000	.1058
74.170	.30070	560.350	390.22000	.1058
74.260	.25050	471.790	-1.00000	.1058
74.300	.25040	476.650	342.77000	.1058
74.350	.20590	393.730	-1.00000	.1058
74.480	.20610	395.510	277.67000	.1058
74.480	.15450	301.250	-1.00000	.1058
74.570	.15530	304.430	209.73000	.1058
74.570	.10070	201.650	-1.00000	.1058
74.570	.10010	204.630	130.67000	.1058
74.840	.40490	543.160	-1.00000	.1417
74.840	.40170	544.080	416.97000	.1417
74.890	.34670	470.370	-1.00000	.1417
74.840	.29760	406.580	-1.00000	.1417
74.890	.30100	412.840	307.45000	.1417
74.890	.25050	344.420	-1.00000	.1417
74.890	.20970	290.710	-1.00000	.1417
74.890	.20870	292.900	213.43000	.1417
74.980	.15820	222.540	-1.00000	.1417
74.930	.10930	156.830	-1.00000	.1417
75.070	.10810	158.400	110.23000	.1417
75.650	.49740	537.670	-1.00000	.1743
75.880	.49780	542.940	420.61000	.1743
76.060	.45050	492.710	-1.00000	.1743
76.100	.40650	446.480	-1.00000	.1743
76.330	.40620	449.200	348.54000	.1743
76.420	.35230	389.420	-1.00000	.1743
76.640	.29880	327.600	-1.00000	.1743
76.780	.30060	334.260	252.53000	.1743
76.870	.24530	274.860	-1.00000	.1743
73.400	.19990	224.180	-1.00000	.1743
77.140	.20030	227.330	168.47000	.1743
77.500	.14710	167.990	-1.00000	.1743
77.810	.10870	126.060	-1.00000	.1743

Temperature, °F	Mass-flow rate, (lbm/sec)*100	Total pressure, psf	Chamber pressure, psf	Valve opening length, in.
77.770	.10890	129.210	91.70000	.1743
77.810	.59550	539.940	-1.00000	.2064
77.500	.60360	551.210	435.18000	.2064
77.270	.50790	466.960	-1.00000	.2064
77.180	.45110	414.840	-1.00000	.2064
77.140	.44990	415.920	327.90000	.2064
77.140	.40250	365.910	-1.00000	.2064
77.050	.35850	329.540	-1.00000	.2064
76.960	.30000	280.530	-1.00000	.2064
76.960	.29880	278.910	212.78000	.2064
76.820	.25440	240.070	-1.00000	.2064
76.910	.19770	184.300	-1.00000	.2064
76.910	.14920	142.390	-1.00000	.2064
76.960	.12570	120.060	-1.00000	.2064
76.910	.12540	123.640	88.06000	.2064
77.270	.71140	545.590	-1.00000	.2529
76.640	.71960	558.340	457.96000	.2529
76.240	.59930	463.460	-1.00000	.2529
75.830	.50480	389.020	-1.00000	.2529
75.520	.50990	395.350	315.93000	.2529
71.600	.45610	350.940	-1.00000	.2529
75.160	.40840	314.600	-1.00000	.2529
74.980	.35860	276.140	-1.00000	.2529
74.930	.29560	229.200	-1.00000	.2529
74.890	.29990	233.180	180.16000	.2529
74.710	.24670	190.380	-1.00000	.2529
74.660	.19900	154.160	-1.00000	.2529
74.710	.15070	116.960	-1.00000	.2529
74.660	.15240	120.240	86.39000	.2529
73.900	.79960	540.090	-1.00000	.2801
73.630	.79090	541.600	452.38000	.2801
73.180	.69930	478.870	-1.00000	.2801
73.000	.60450	412.260	-1.00000	.2801
72.680	.60500	412.040	337.02000	.2801
72.050	.49910	335.300	-1.00000	.2801
71.960	.45160	303.200	-1.00000	.2801
72.010	.45640	308.720	245.18000	.2801
72.050	.40040	269.360	-1.00000	.2801
72.050	.35320	238.020	-1.00000	.2801
72.190	.29840	200.450	-1.00000	.2801
72.280	.29910	203.100	156.63000	.2801
72.460	.24810	165.810	-1.00000	.2801
72.500	.20620	139.390	-1.00000	.2801
72.680	.18090	121.040	-1.00000	.2801

Temperature, °F	Mass-flow rate, (lbm/sec)*100	Total pressure, psf	Chamber pressure, psf	Valve opening length, in.
72.770	.18070	123.660	88.52000	.2801
72.010	.90100	535.290	-1.00000	.3171
71.740	.90720	541.330	453.29000	.3171
71.060	.79470	470.420	-1.00000	.3171
70.700	.69890	411.810	-1.00000	.3171
70.610	.69870	413.270	341.41000	.3171
70.340	.60910	358.030	-1.00000	.3171
70.340	.51020	298.890	-1.00000	.3171
70.340	.39070	228.960	-1.00000	.3171
70.430	.38960	230.770	183.01000	.3171
70.480	.29900	176.530	-1.00000	.3171
70.570	.20040	117.850	-1.00000	.3171
70.750	.20030	120.480	86.76000	.3171
70.210	1.00060	545.890	-1.00000	.3401
69.940	.99920	548.620	460.18000	.3401
69.440	.90390	488.390	-1.00000	.3401
69.310	.79200	430.470	-1.00000	.3401
69.310	.69450	376.560	-1.00000	.3401
69.220	.69630	378.790	309.93000	.3401
69.170	.60700	327.360	-1.00000	.3401
69.350	.50200	271.640	-1.00000	.3401
69.490	.39670	213.430	-1.00000	.3401
69.580	.39570	215.080	170.98000	.3401
69.800	.29610	159.260	-1.00000	.3401
69.980	.22160	119.740	-1.00000	.3401
70.210	.22330	121.990	87.15000	.3401
76.460	1.09280	532.660	-1.00000	.3687
76.060	1.08250	532.830	448.46000	.3687
75.740	1.00710	493.730	-1.00000	.3687
75.380	.90540	442.460	-1.00000	.3687
75.250	.89920	441.520	368.74000	.3687
74.980	.80300	391.540	-1.00000	.3687
74.840	.69610	339.500	-1.00000	.3687
74.800	.60660	294.860	-1.00000	.3687
74.710	.60180	295.190	240.73000	.3687
74.530	.49890	243.150	-1.00000	.3687
74.530	.39840	193.890	-1.00000	.3687
74.530	.30590	149.980	-1.00000	.3687
74.480	.30590	151.510	113.06000	.3687
74.530	.24650	120.820	-1.00000	.3687
74.530	.24600	122.720	87.75000	.3687
70.970	1.19760	479.730	-1.00000	.4411
70.840	1.19250	484.240	399.56000	.4411
69.980	1.00820	413.650	-1.00000	.4411

Temperature, ^{o}F	Mass-flow rate, (lbm/sec)*100	Total pressure, psf	Chamber pressure, psf	Valve opening length, in.
69.760	.80570	331.200	-1.00000	.4411
69.620	.80280	331.880	271.73000	.4411
69.220	.82910	338.420	-1.00000	.4411
69.040	.84020	344.630	281.78000	.4411
68.720	.70700	289.270	-1.00000	.4411
68.720	.59920	246.060	-1.00000	.4411
68.680	.59990	248.400	198.41000	.4411
68.680	.50150	206.740	-1.00000	.4411
68.770	.40120	166.060	-1.00000	.4411
68.900	.30610	130.250	-1.00000	.4411
69.040	.30730	133.060	99.84000	.4411
69.670	1.19540	432.300	-1.00000	.4789
69.490	1.18660	435.410	356.50000	.4789
68.990	1.00060	371.450	-1.00000	.4789
68.770	.80100	298.580	-1.00000	.4789
68.680	.80040	300.890	243.97000	.4789
68.500	.69720	260.660	-1.00000	.4789
68.500	.60200	225.400	-1.00000	.4789
68.410	.60030	227.040	180.60000	.4789
69.490	.50870	190.460	-1.00000	.4790
69.490	.40550	153.840	-1.00000	.4789
69.580	.30010	123.570	-1.00000	.4789
69.620	.30060	126.670	98.88000	.4789
76.330	1.20620	398.100	-1.00000	.5100
76.510	1.19250	400.100	324.45000	.5100
75.970	1.00960	342.500	-1.00000	.5100
75.700	.79380	269.530	-1.00000	.5100
75.520	.79740	272.380	218.08000	.5100
75.070	.60790	208.590	-1.00000	.5100
74.840	.40950	143.030	-1.00000	.5100
74.750	.40880	144.760	110.43000	.5100

TEST DATA FOR 3/4-INCH VALVE AT -30°F

Temperature, °F	Mass-flow rate, (lbm/sec)*100	Total pressure, psf	Chamber pressure, psf	Valve opening length, in.
-35.360	.19314	405.000	-1.00000	.0902
-31.180	.19248	411.550	217.49000	.0902
-31.360	.41699	397.850	-1.00000	.1708
-29.140	.41016	391.920	244.64554	.1708
-21.500	.20877	206.950	-1.00000	.1708
-18.040	.21174	210.680	125.34227	.1708
-33.640	.61938	394.900	-1.00000	.2360
-32.710	.62156	399.050	300.26392	.2360
-26.090	.40474	270.440	-1.00000	.2360
-24.520	.40824	273.140	198.20537	.2360
-20.420	.30418	205.760	-1.00000	.2360
-17.500	.30859	209.380	149.20564	.2360
-28.360	.82390	394.320	-1.00000	.3068
-26.950	.83215	402.620	327.73894	.3068
-22.720	.62866	303.130	-1.00000	.3068
-20.650	.63114	305.050	238.14920	.3068
-29.560	.40431	214.540	166.36902	.3068
-53.860	.83790	305.090	-1.00000	.3772
-54.580	.84907	307.550	250.56566	.3772
-53.140	.63456	232.230	-1.00000	.3772
-51.200	.63722	233.760	185.41817	.3772
-47.380	.81920	250.010	-1.00000	.4474
-47.920	.81648	252.410	203.96000	.4474

TEST DATA FOR 3/4-INCH VALVE AT 10°F

Temperature, °F	Mass-flow rate, (lbm/sec)*100	Total pressure, psf	Chamber pressure, psf	Valve opening length, in.
5.630	.10215	393.760	-1.00000	.0538
11.790	.10397	409.300	208.28000	.0538
6.170	.21044	409.550	-1.00000	.0975
8.730	.21231	414.310	181.94000	.0975
6.210	.41871	393.710	-1.00000	.1764
7.290	.42202	396.970	255.39288	.1764
11.250	.21267	212.860	-1.00000	.1764
14.040	.21170	213.080	121.75405	.1764
12.620	.63305	402.810	-1.00000	.2459
14.000	.63570	404.900	301.23456	.2459
16.830	.41559	268.770	-1.00000	.2459
17.820	.41904	272.500	197.68182	.2459
19.490	.27729	191.320	-1.00000	.2459
20.750	.27905	193.110	135.49959	.2459
2.390	.82187	404.050	-1.00000	.3066
4.860	.82365	407.510	326.42333	.3066
9.090	.62626	308.870	-1.00000	.3066
10.670	.63029	311.330	242.39069	.3066
14.040	.40838	205.460	-1.00000	.3066
15.300	.41222	207.830	152.93134	.3066
-.530	.82714	335.430	-1.00000	.3662
-.160	.82850	336.860	271.60530	.3662
1.800	.62739	255.960	-1.00000	.3662
3.150	.63108	257.820	204.68542	.3662
5.940	.46591	191.860	-1.00000	.3662
6.980	.46824	193.020	147.44225	.3662
-3.500	.82422	280.000	-1.00000	.4277
-2.870	.83728	285.150	230.67515	.4277
-1.120	.61806	210.330	-1.00000	.4277
.620	.62041	211.530	167.37187	.4277
4.370	.82419	243.130	-1.00000	.4874
5.540	.82210	244.810	197.05000	.4874

TEST DATA FOR 3/4-INCH VALVE AT 75°F

Temperature, °F	Mass-flow rate, (lbm/sec)*100	Total pressure, psf	Chamber pressure, psf	Valve opening length, in.
75.150	.59200	542.290	-1.00000	.1780
74.930	.59500	550.720	362.52000	.1780
74.700	.50400	471.130	-1.00000	.1780
74.660	.45800	427.420	-1.00000	.1780
74.520	.45800	432.040	281.82000	.1780
74.390	.40300	375.180	-1.00000	.1780
74.300	.36000	340.430	-1.00000	.1780
74.840	.30800	288.150	-1.00000	.1780
74.750	.30800	292.350	184.14000	.1780
74.250	.25900	246.250	-1.00000	.1780
74.300	.21000	201.320	-1.00000	.1780
74.390	.21300	206.240	126.50000	.1780
74.390	.15300	148.680	-1.00000	.1780
74.610	.10300	102.150	-1.00000	.1780
74.790	.10200	105.270	63.45000	.1780
74.120	.69300	543.570	-1.00000	.2057
73.760	.69200	548.220	388.33000	.2057
73.440	.60700	480.750	-1.00000	.2057
72.860	.49700	395.460	-1.00000	.2057
72.720	.49800	398.050	271.55000	.2057
72.630	.45000	357.580	-1.00000	.2057
72.590	.39200	313.400	-1.00000	.2057
72.630	.34200	273.290	-1.00000	.2057
72.630	.29600	237.520	-1.00000	.2057
72.720	.29700	240.990	155.65000	.2057
72.810	.25700	204.880	-1.00000	.2057
72.900	.20200	164.340	-1.00000	.2057
72.900	.15700	129.750	-1.00000	.2057
71.190	.80400	534.000	-1.00000	.2383
71.010	.80800	538.400	397.53000	.2383
70.790	.70100	467.580	-1.00000	.2383
70.700	.60200	403.400	-1.00000	.2383
70.560	.60300	404.290	290.82000	.2383
70.380	.50800	339.940	-1.00000	.2383
70.380	.45000	301.710	-1.00000	.2383
70.290	.45100	303.770	212.49000	.2383
70.290	.39800	266.310	-1.00000	.2383
70.290	.35400	235.760	-1.00000	.2383
70.250	.30900	207.170	-1.00000	.2383
70.250	.31200	209.720	140.03000	.2383
70.200	.25700	171.810	-1.00000	.2383
70.290	.20700	139.250	-1.00000	.2383

Temperature, °F	Mass-flow rate, (lbm/sec)*100	Total pressure, psf	Chamber pressure, psf	Valve opening length, in.
70.200	.15600	105.560	-1.00000	.2383
73.890	.89300	541.560	-1.00000	.2629
73.620	.88500	539.110	407.96000	.2629
73.260	.79400	484.640	-1.00000	.2629
73.080	.70800	434.050	-1.00000	.2629
72.860	.70500	432.860	320.89000	.2629
72.630	.60100	369.150	-1.00000	.2629
72.360	.49700	305.760	-1.00000	.2629
72.270	.40900	253.230	-1.00000	.2629
72.180	.40900	254.560	178.88000	.2629
72.050	.29900	185.920	-1.00000	.2629
72.050	.19700	123.930	-1.00000	.2629
72.050	.19700	125.960	82.86000	.2629
71.510	.99400	540.230	-1.00000	.2940
71.240	.99200	543.430	417.68000	.2940
70.830	.90200	494.840	-1.00000	.2940
70.700	.79700	439.290	-1.00000	.2940
70.560	.69700	386.020	-1.00000	.2940
70.430	.69100	383.980	287.28000	.2940
70.290	.59900	331.860	-1.00000	.2940
70.250	.50800	283.020	-1.00000	.2940
70.200	.40500	226.570	-1.00000	.2940
70.250	.40300	226.650	161.60000	.2940
70.200	.30300	171.380	-1.00000	.2940
70.290	.20900	119.060	-1.00000	.2940
70.340	.20900	120.190	80.68000	.2940
70.110	1.11300	533.530	-1.00000	.3264
69.750	1.09200	528.120	415.16000	.3264
69.530	1.00600	486.930	-1.00000	.3264
69.440	.89500	434.950	-1.00000	.3264
74.520	.89200	429.720	331.20000	.3264
74.520	.79700	385.200	-1.00000	.3264
74.430	.70600	342.790	-1.00000	.3264
74.340	.60500	295.670	-1.00000	.3264
74.250	.60300	295.670	221.36000	.3264
74.030	.50600	248.480	-1.00000	.3264
73.980	.40300	199.020	-1.00000	.3264
73.850	.30100	149.850	-1.00000	.3264
73.710	.29700	148.920	105.40000	.3264
73.530	.24300	120.860	-1.00000	.3264
73.490	.24300	122.220	83.18000	.3264
74.390	1.20800	537.530	-1.00000	.3438
67.140	1.21000	532.290	-1.00000	.3438
66.510	1.20800	531.350	423.50000	.3438

Temperature, ^{o}F	Mass-flow rate, (lbm/sec)*100	Total pressure, psf	Chamber pressure, psf	Valve opening length, in.
65.340	1.01000	441.510	-1.00000	.3438
65.250	.79500	349.100	-1.00000	.3438
65.300	.79300	348.830	271.36000	.3438
65.340	.70200	308.800	-1.00000	.3438
65.700	.59500	261.540	-1.00000	.3438
65.880	.59600	262.630	199.59000	.3438
66.150	.49800	219.420	-1.00000	.3438
66.510	.39800	176.360	-1.00000	.3438
67.370	.29800	131.950	-1.00000	.3438
67.770	.30000	133.930	95.06000	.3438
68.670	.27400	120.040	-1.00000	.3438
68.810	.27400	121.890	85.55000	.3438
74.120	1.19600	480.360	-1.00000	.3833
74.350	1.18300	484.630	385.75000	.3833
74.170	1.00700	416.040	-1.00000	.3833
73.940	.80400	334.400	-1.00000	.3833
73.710	.81000	336.780	262.40000	.3833
73.220	.71300	295.830	-1.00000	.3833
73.170	.60600	252.930	-1.00000	.3833
73.040	.60300	251.460	192.12000	.3833
72.900	.50600	210.300	-1.00000	.3833
72.900	.40200	167.670	-1.00000	.3833
72.950	.30300	126.930	-1.00000	.3833
73.040	.30500	127.980	92.26000	.3833
73.350	1.20400	459.370	-1.00000	.4002
72.810	1.19000	459.400	375.36000	.4002
71.820	.99300	383.430	-1.00000	.4002
71.510	.79200	307.310	-1.00000	.4002
71.100	.82300	318.720	251.34000	.4002
70.830	.60000	232.620	-1.00000	.4002
70.880	.40300	157.390	-1.00000	.4002
70.920	.40600	158.690	118.85000	.4002
71.060	.32000	123.610	-1.00000	.4002
71.150	.32000	124.470	90.05000	.4002
71.420	1.20300	431.350	-1.00000	.4223
71.150	1.19600	433.470	349.01000	.4223
70.790	.99700	362.990	-1.00000	.4223
70.650	.80600	294.990	-1.00000	.4223
70.610	.80600	294.870	231.41000	.4223
70.520	.60300	221.060	-1.00000	.4223
70.470	.40600	149.350	-1.00000	.4223
70.560	.40200	148.940	111.32000	.4223
70.650	.33800	123.970	-1.00000	.4223
70.740	.33700	124.270	91.10000	.4223

Temperature, °F	Mass-flow rate, (lbm/sec)*100	Total pressure, psf	Chamber pressure, psf	Valve opening length, in.
71.510	1.20400	387.400	-1.00000	.4688
71.280	1.19100	387.290	310.25000	.4688
70.920	.99400	325.020	-1.00000	.4688
70.880	.79500	261.650	-1.00000	.4688
70.790	.78700	259.310	204.18000	.4688
70.700	.60600	199.940	-1.00000	.4688
70.740	.40800	135.340	-1.00000	.4688
70.790	.40500	135.260	100.96000	.4688
71.010	1.19900	348.430	-1.00000	.5187
70.880	1.18100	344.870	275.81000	.5187
70.610	1.00500	295.170	-1.00000	.5187
70.520	.79200	233.440	-1.00000	.5187
70.470	.76400	227.020	179.10000	.5187

References

1. Fischer, M. C.; Wright, A. S., Jr.; and Wagner, R. D.: A Flight Test of Laminar Flow Control Leading-Edge Systems. AIAA-83-2508, Oct. 1983.
2. Wagner, Richard D.; and Fischer, Michael C.: Developments in the NASA Transport Aircraft Laminar Flow Program. AIAA-83-0090, Jan. 1983.
3. Blackburn, John F.; Reethof, Gerhard; and Shearer, J. Lowen, eds.: *Fluid Power Control.* Technology Press of M.I.T. and John Wiley & Sons, Inc., c.1960.
4. Holman, J. P.: *Experimental Methods for Engineers,* Second ed. McGraw-Hill, Inc., c.1971.

TABLE 1. VISCOSITY TABLES FOR AIR AND NITROGEN

T, °R	Viscosity, lbm/ft-sec, for—	
	Air	Nitrogen
360	8.7×10^{-6}	8.65×10^{-6}
460	10.8×10^{-6}	10.55×10^{-6}
560	12.7×10^{-6}	12.30×10^{-6}

TABLE 2. x_o AND Δx_p FOR EACH FLIGHT VALVE WHERE $p_v \approx 100$ psfa

[Total of 41 valves]

Valve	Chamber 1		Chamber 3		Chamber 5	
	x_o, in. ($p_c = p_v$)	Δx_p, in. ($\Delta p = 1$ atm $- p_v$)	x_o, in. ($p_c = p_v$)	Δx_p, in. ($\Delta p = 1$ atm $- p_v$)	x_o, in. ($p_c = p_v$)	Δx_p, in. ($\Delta p = 1$ atm $- p_v$)
1	−0.0002	0.0054	(a)		−0.0031	0.0051
2	.0021	.0084	0.0010	0.0075	.0003	.0094
3	−.0040	.0049	−.0035	.0035	.0002	.0051
4	−.0011	.0043	−.0019	.0035	−.0035	.0059
5	.0018	.0093	−.0025	.0060	.0040	.0074
6	−.0011	.0042	−.0004	.0039	−.0008	.0046
7	−.0008	.0042	(a)		−.0048	.0046
8	.0002	.0112	.0029	.0089	.0015	.0083
9	.0013	.0044	.0007	.0032	−.0001	.0048
10	−.0007	.0044	−.0087	.0044	−.0001	.0051
11	.0030	.0088	.0035	.0075	.0005	.0090
12	−.0004	.0065	.0008	.0037	.0011	.0071
13	−.0034	.0050	.0004	.0055	(a)	
14	−.0006	.0085	.0013	.0082	(a)	
15	−.0011	.0055	−.0005	.0061	−.0017	.0051

[a]Valve not located in this position.

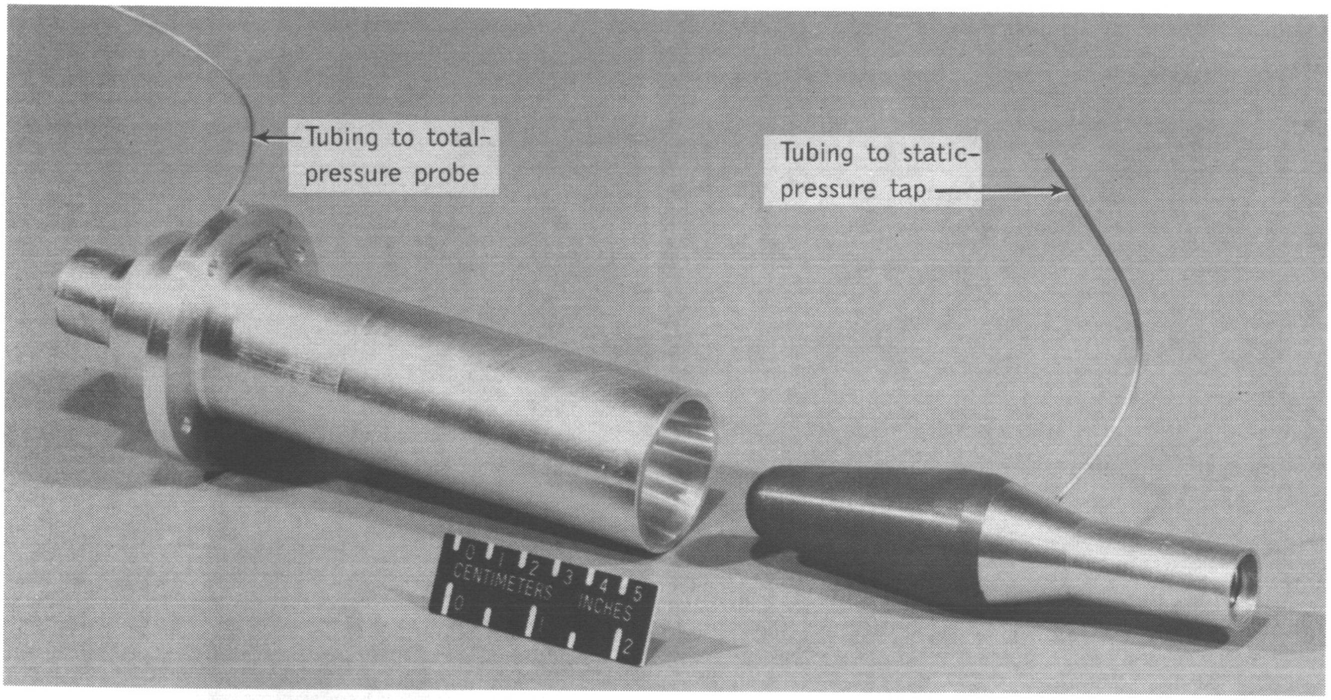

L-85-01

(a) The 3/4-inch valve.

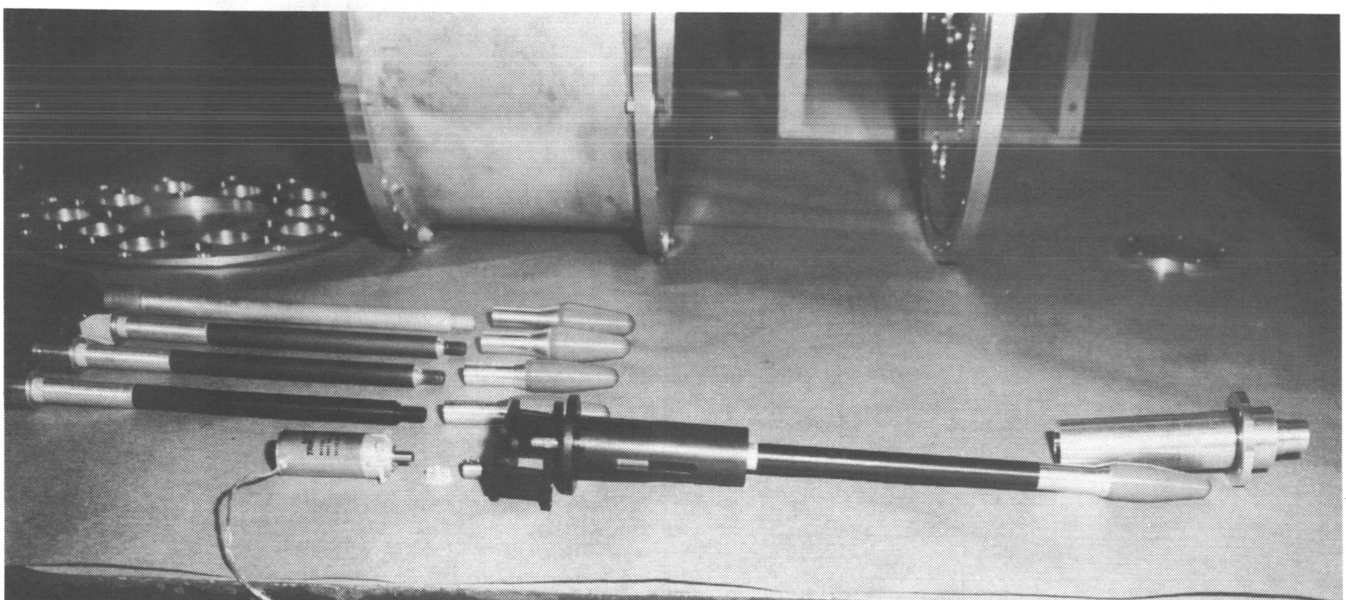

L-82-9500

(b) Typical flight plenum chamber and sonic valve components.

Figure 1. Left suction system components.

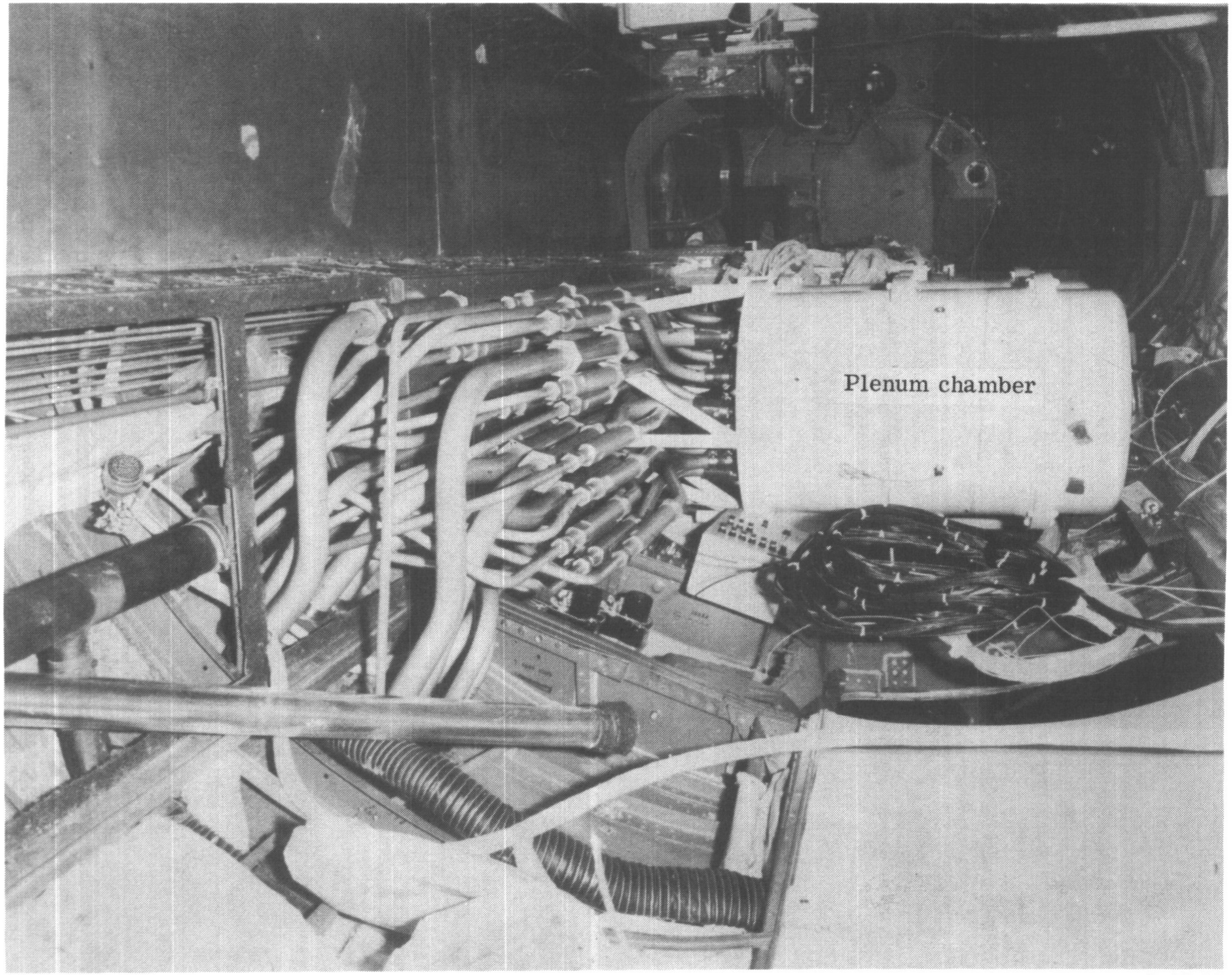

L-85-02

(c) Plenum chamber as installed in JetStar aircraft.

Figure 1. Continued.

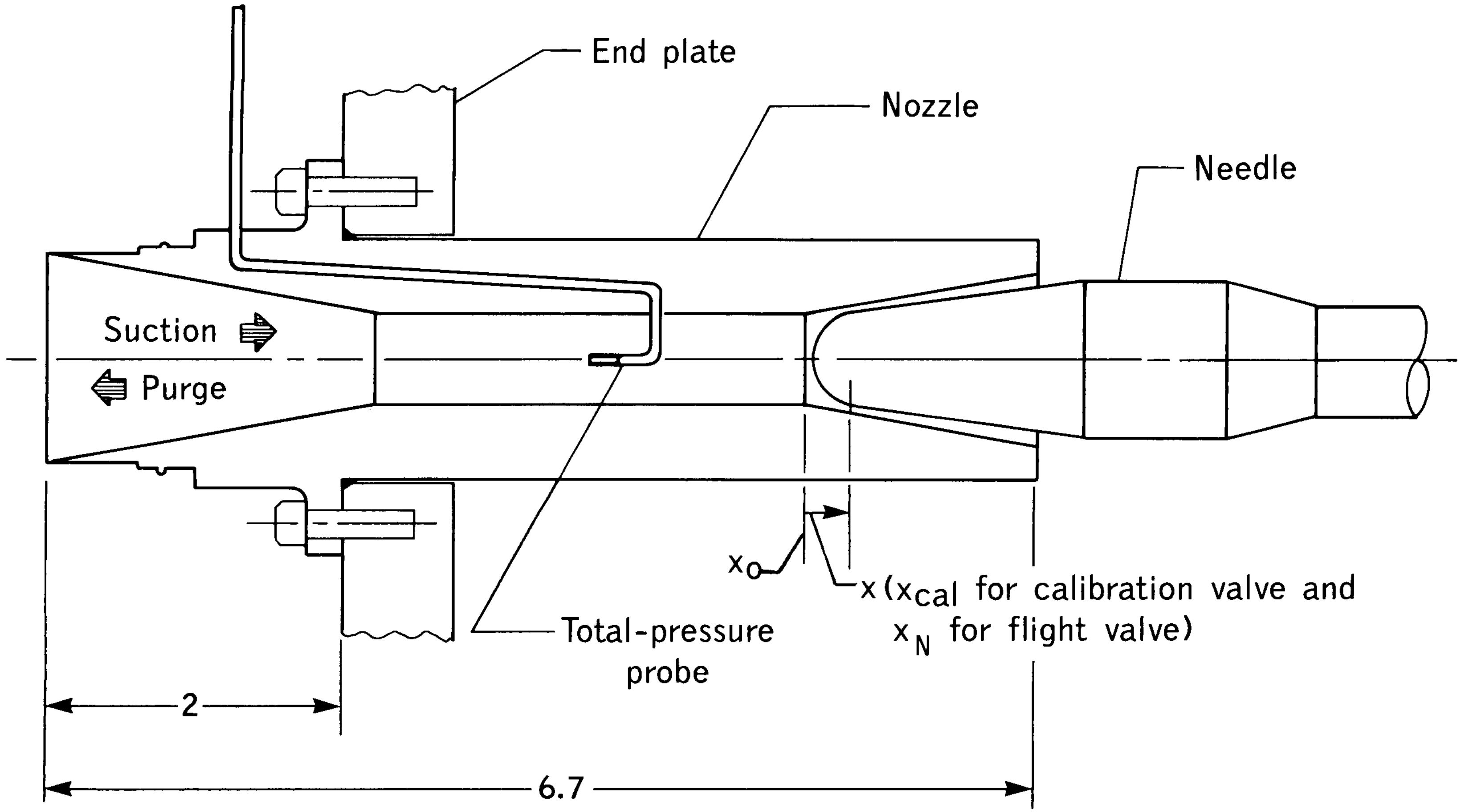

(d) The 5/8-inch flight valve mounted on end plate. Linear dimensions are in inches.

Figure 1. Concluded.

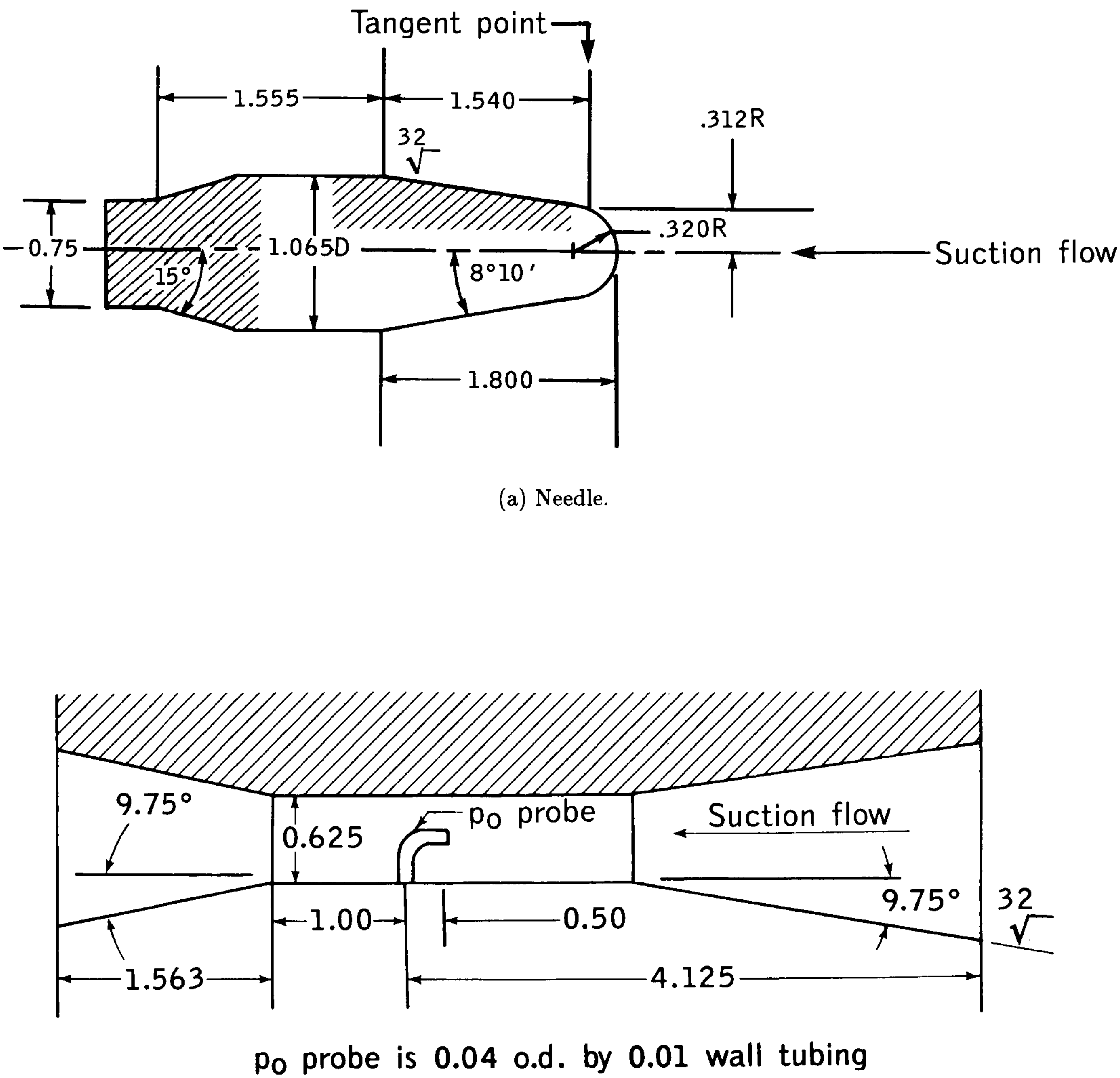

(a) Needle.

(b) Nozzle.

Figure 2. Section views of components of 5/8-inch valve. Linear dimensions are in inches.

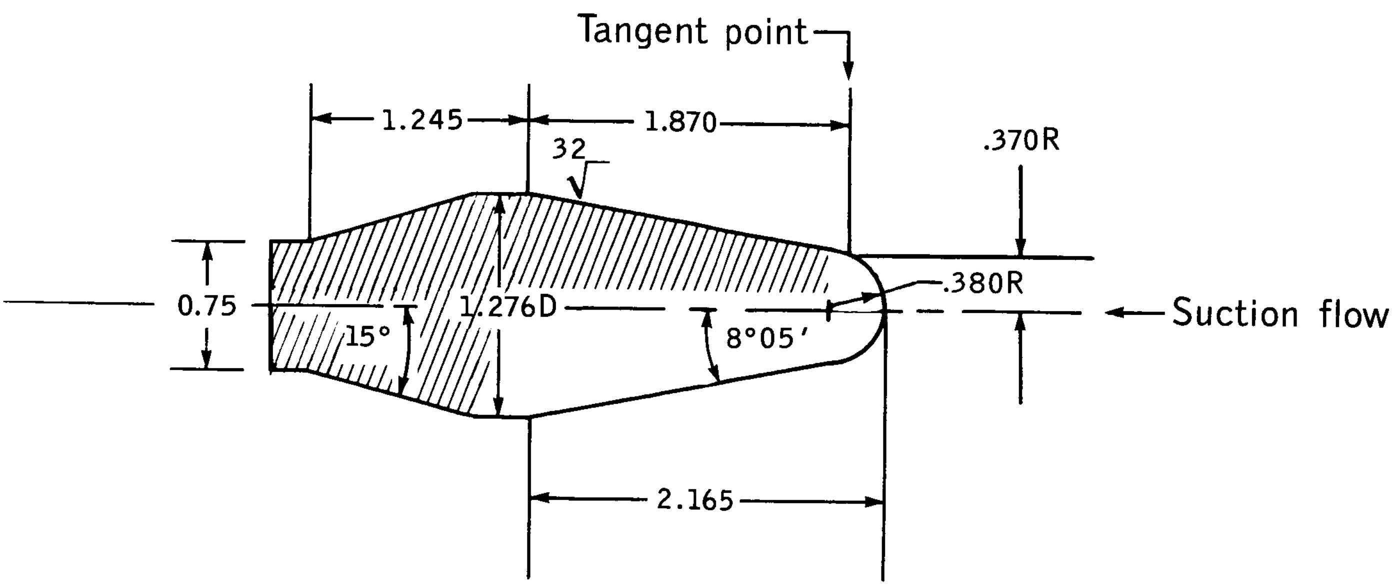

(a) Needle.

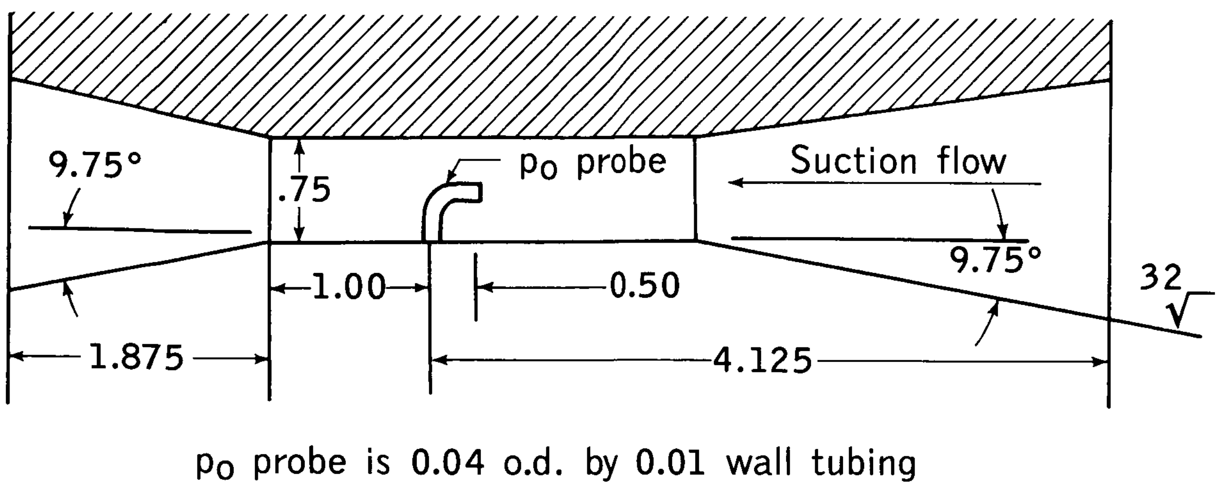

(b) Nozzle.

Figure 3. Section views of components of 3/4-inch valve. Linear dimensions are in inches.

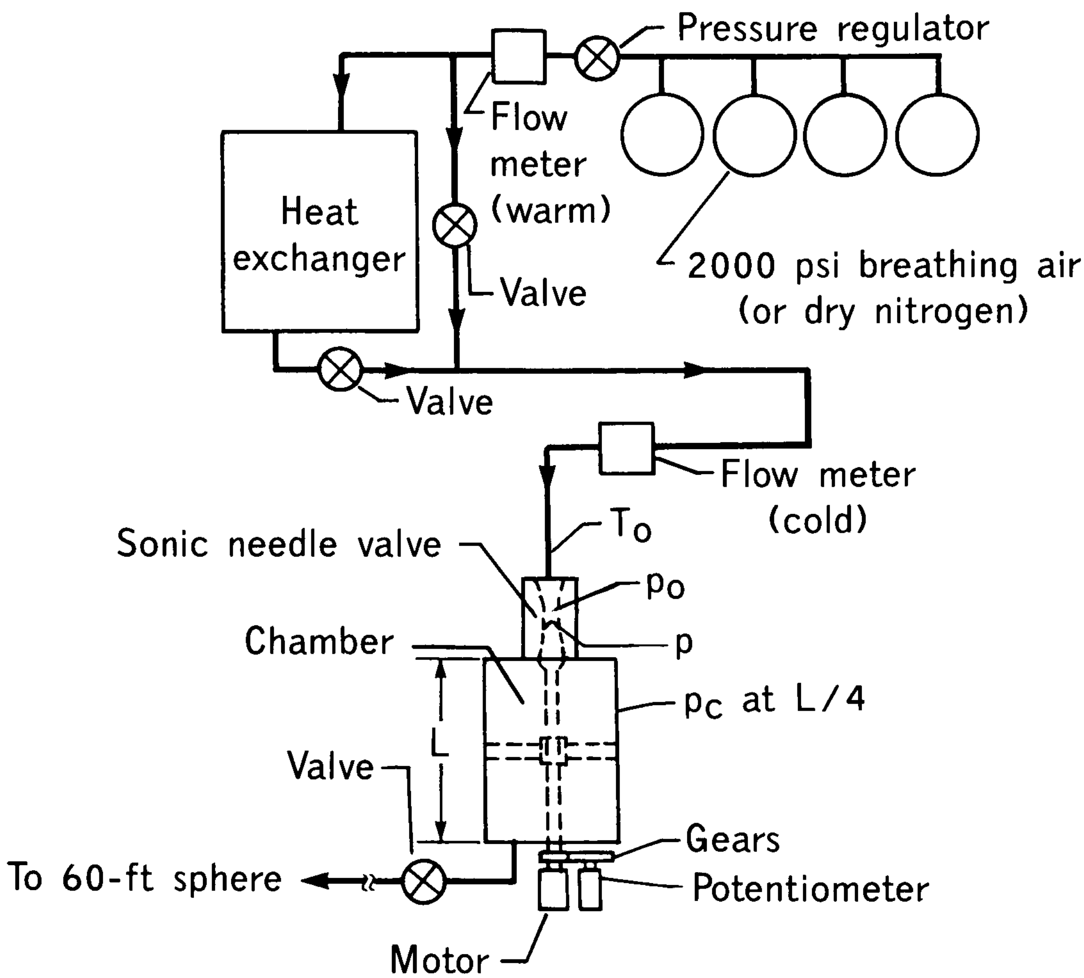

Figure 4. Schematic diagram of test fixture.

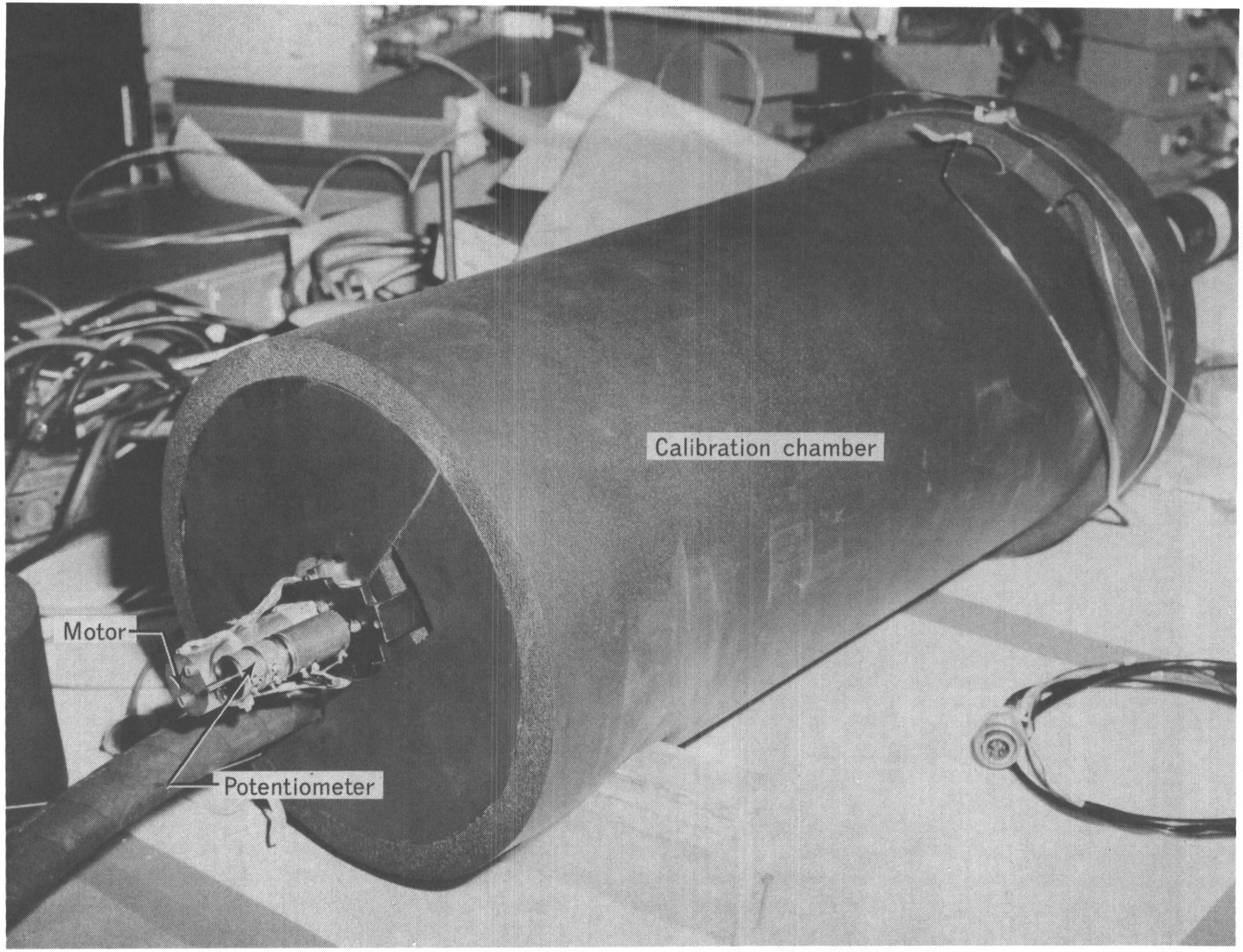

L-85-03

Figure 5. Calibration chamber with needle drive motor and rotary potentiometer.

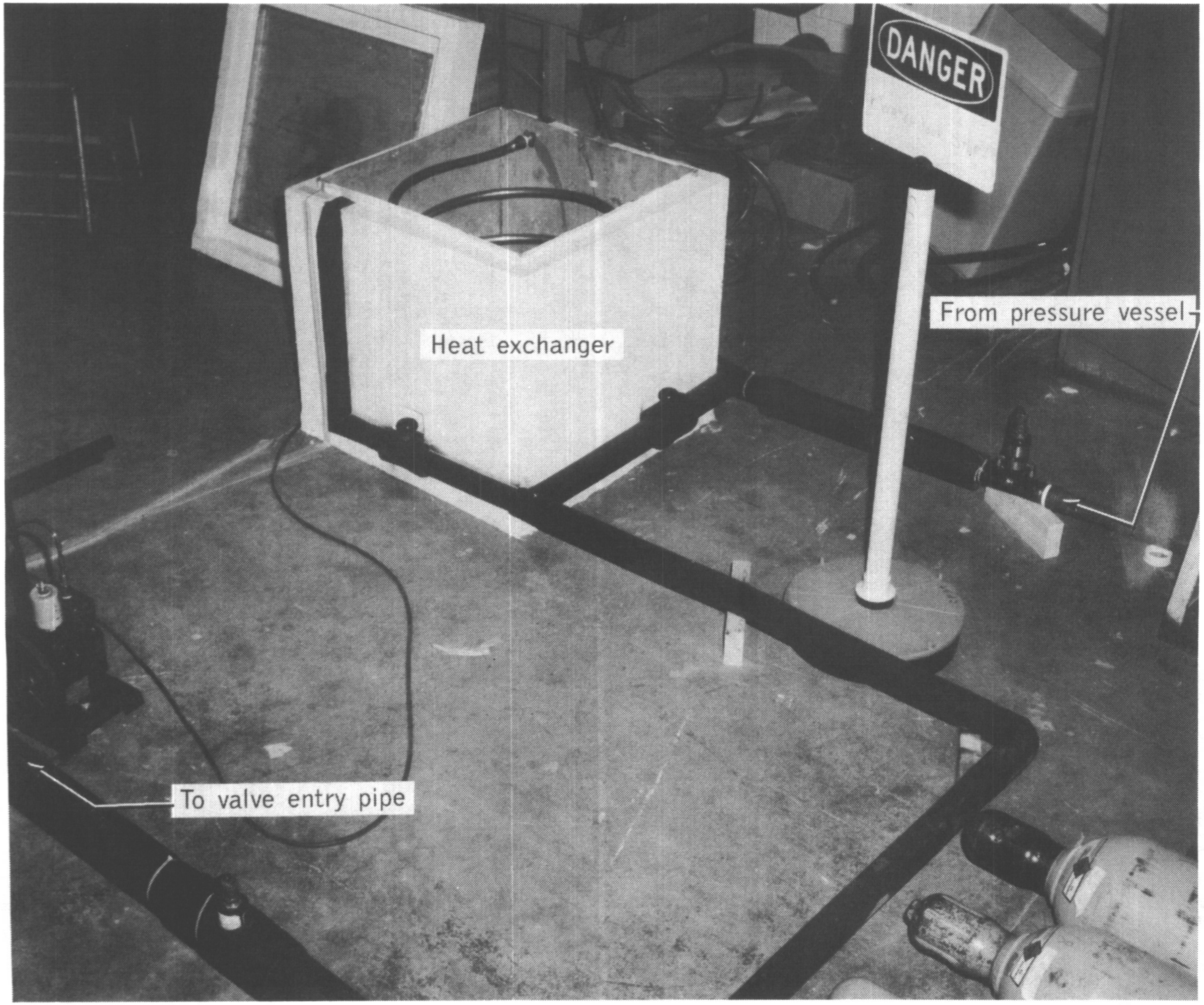

L-85-04

Figure 6. Flow system from pressure vessel to valve entry pipe.

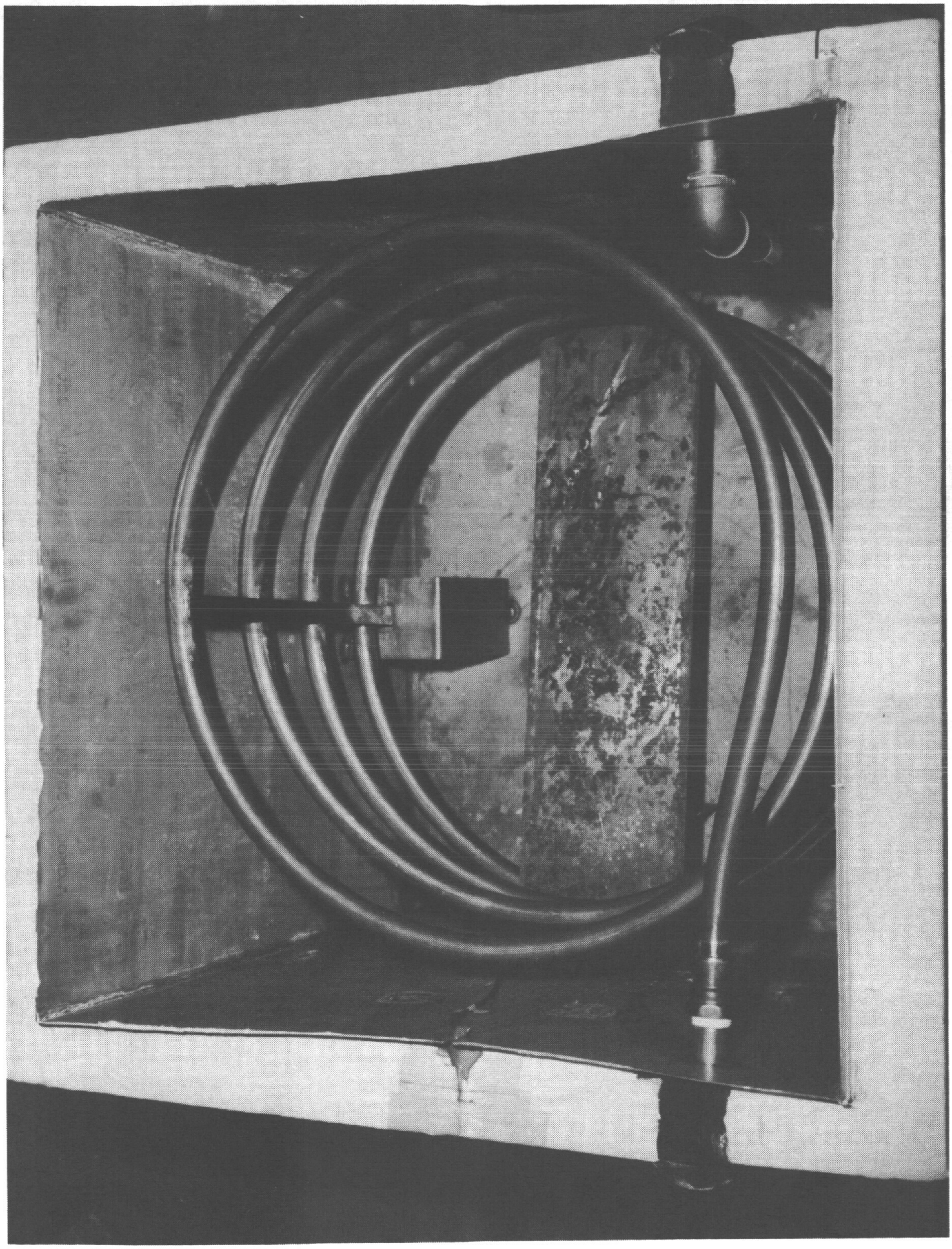

L-82-11,653

Figure 7. Heat exchanger.

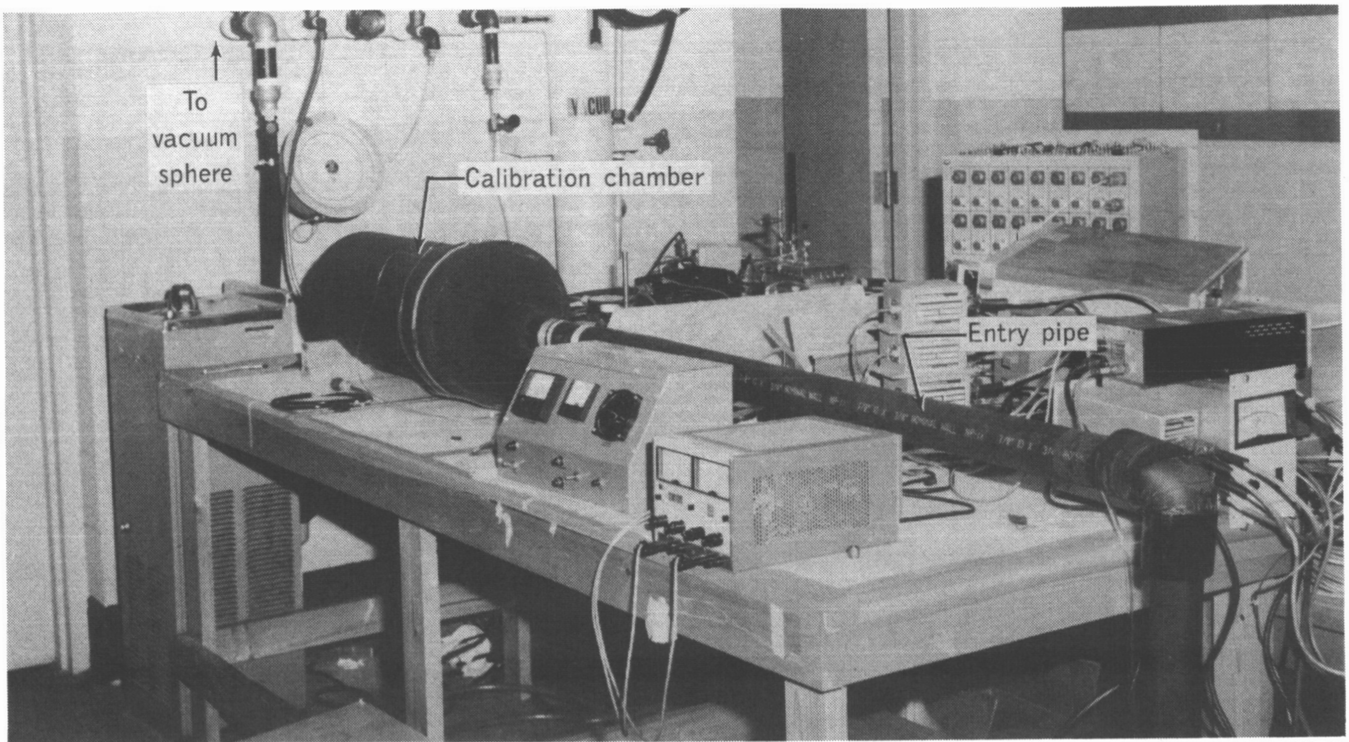

L-85-05

Figure 8. Flow system from entry pipe to vacuum sphere connection.

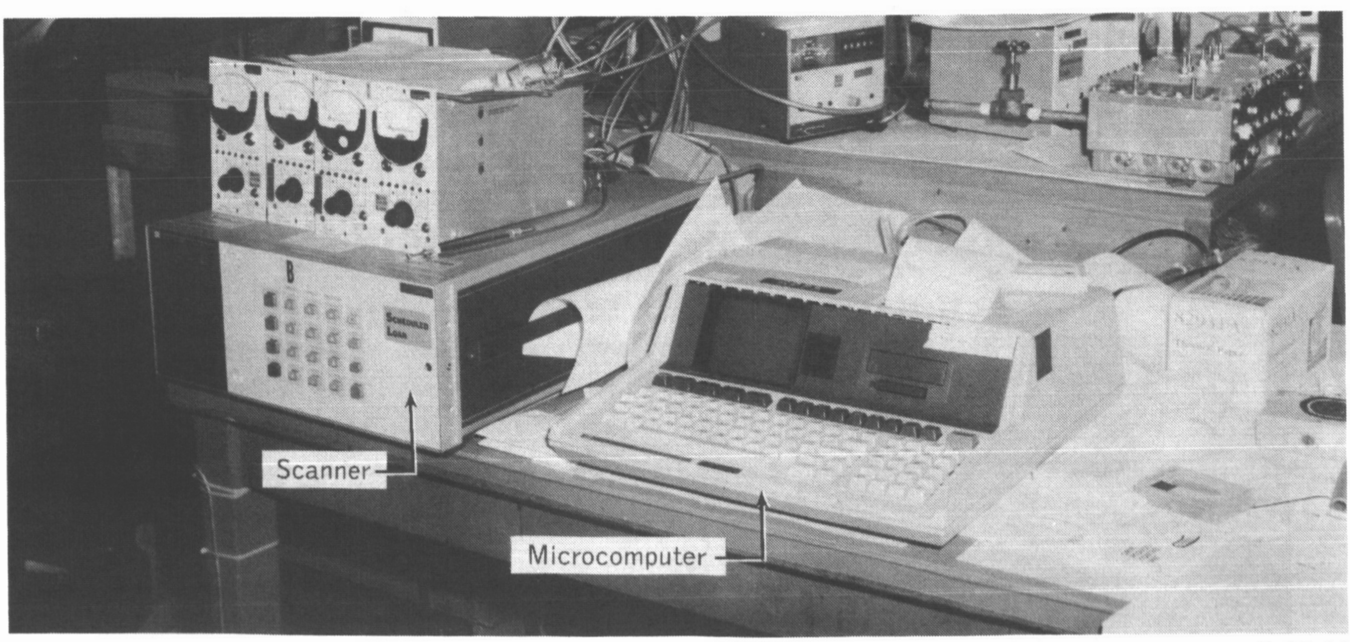

L-85-06

Figure 9. Signal scanner and microcomputer.

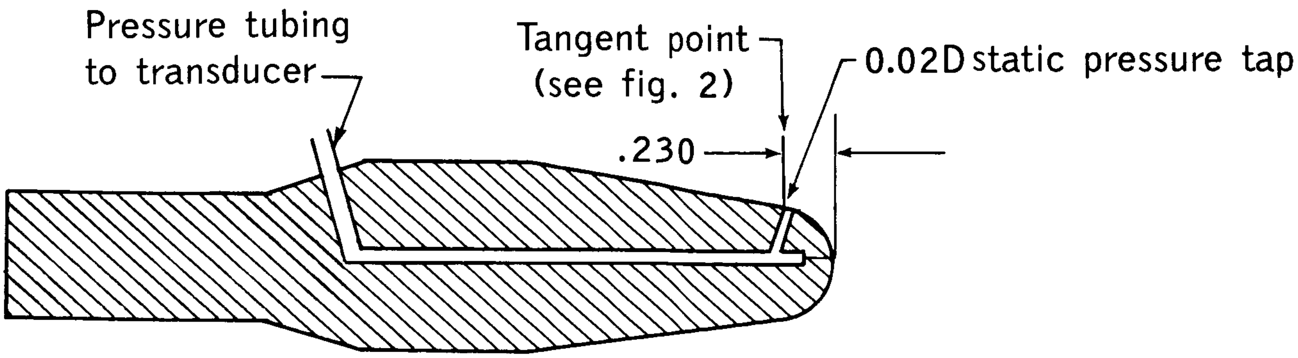

5/8-inch calibration needle

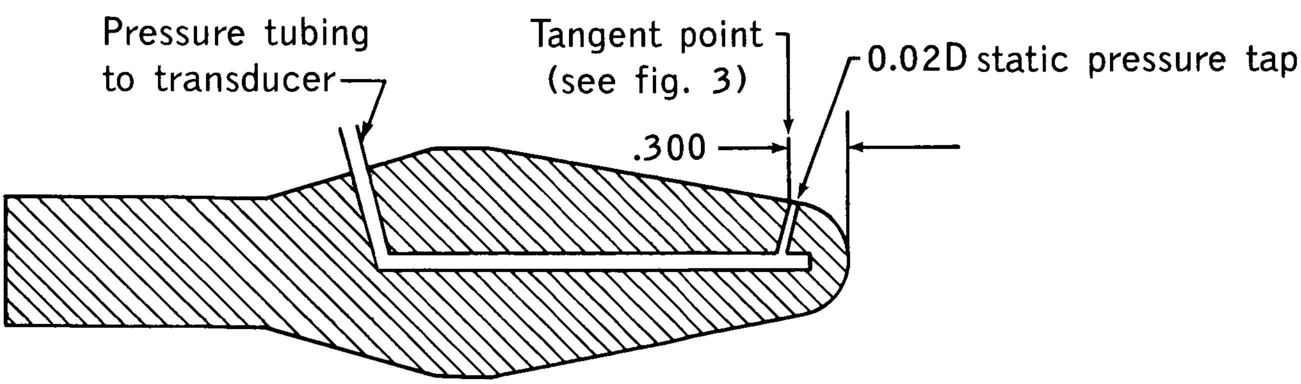

3/4-inch calibration needle

Figure 10. Throat pressure taps. Linear dimensions are in inches.

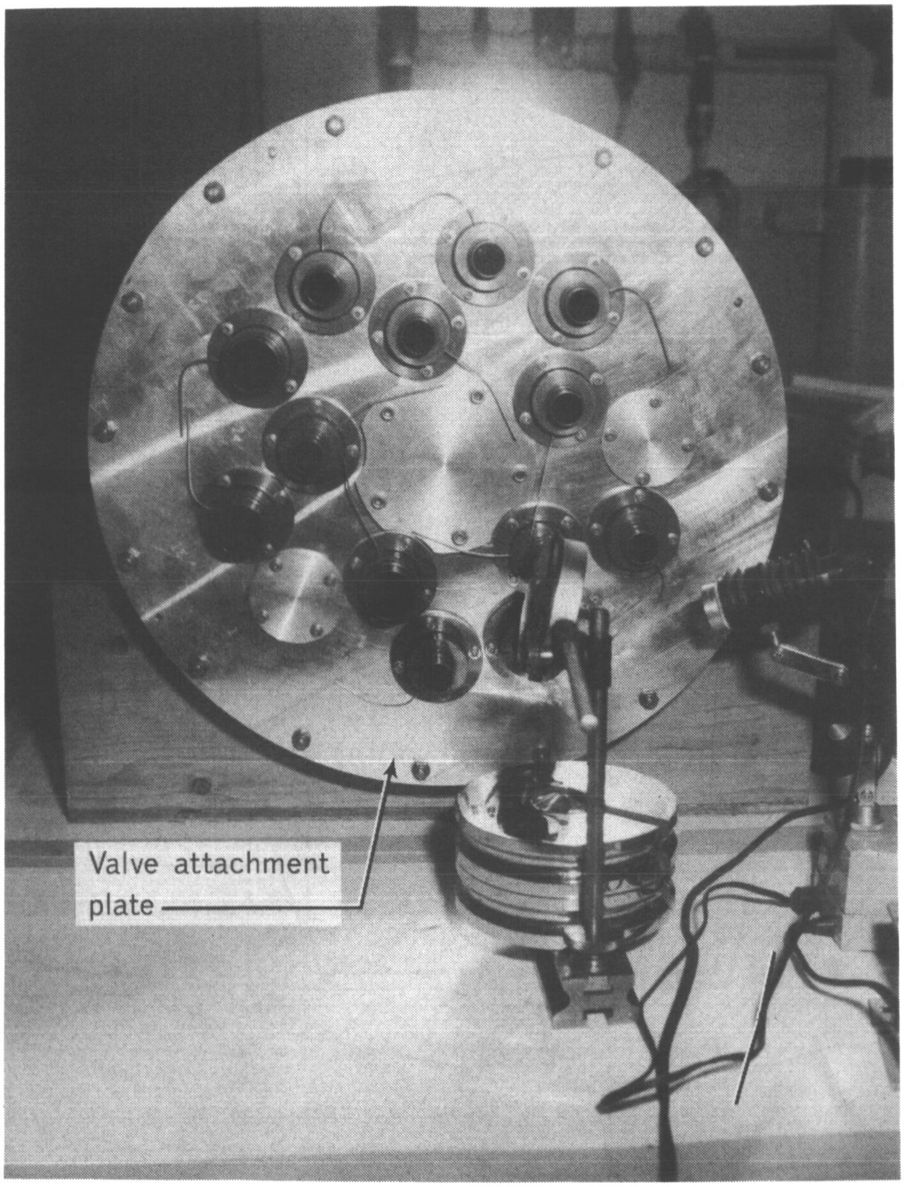

L-85-07

Figure 11. Sonic valves installed in flight chamber.

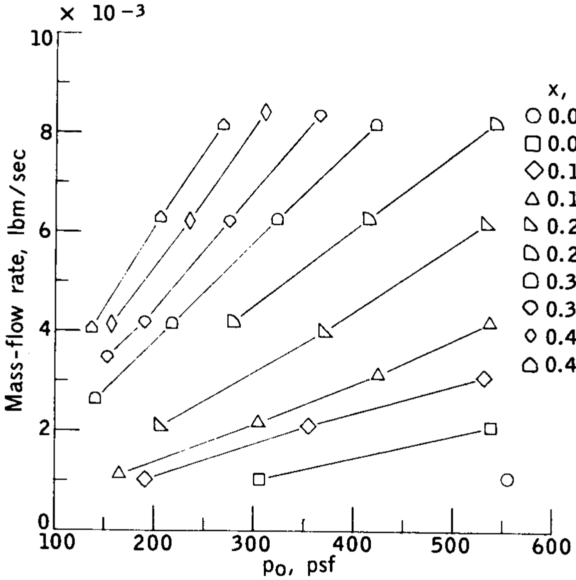

(a) Temperature, −30°F.

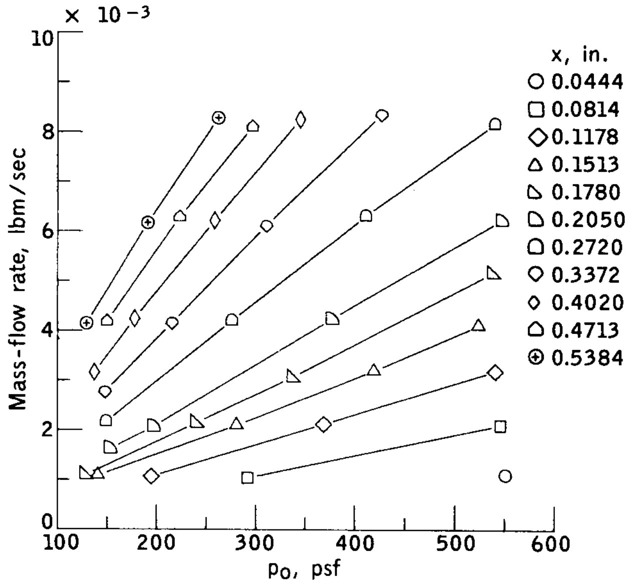

(b) Temperature, 10°F.

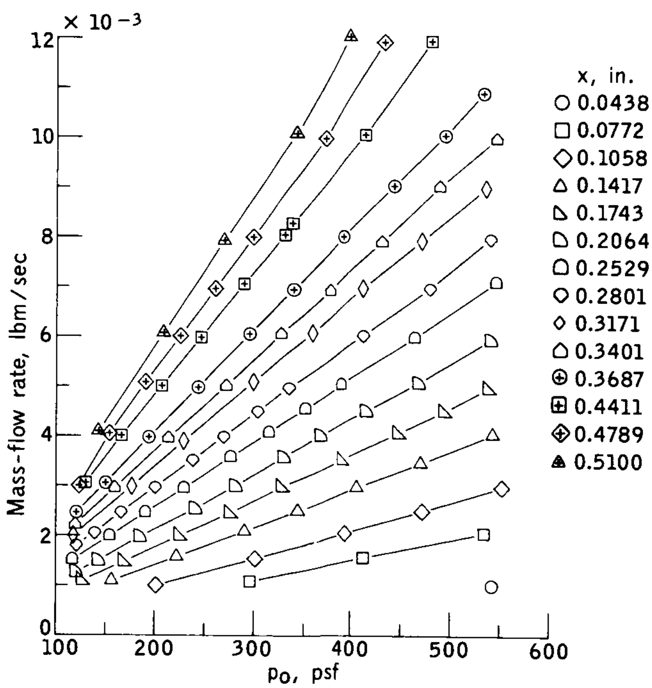

(c) Temperature, 75°F.

Figure 12. Mass-flow-rate data for 5/8-inch calibration valve.

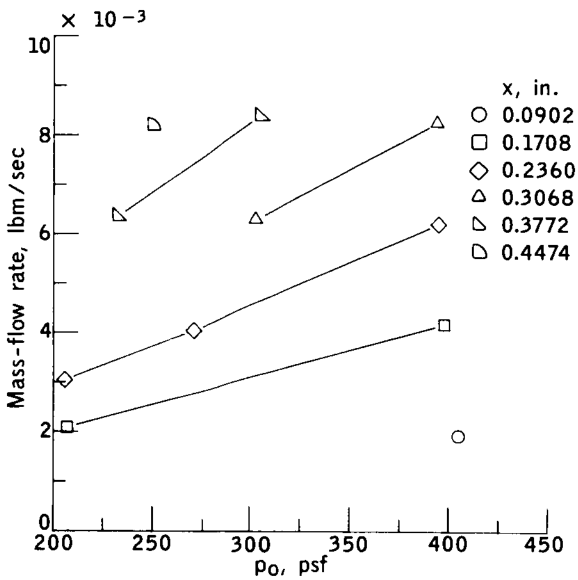

(a) Temperature, −30°F.

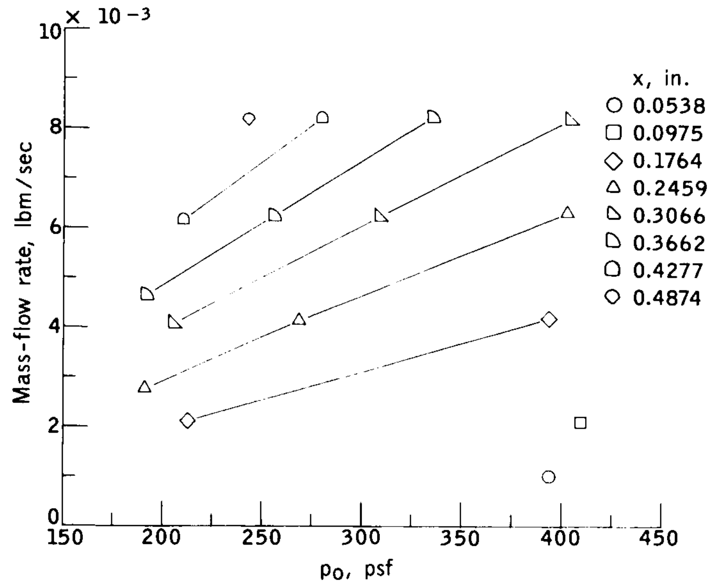

(b) Temperature, 10°F.

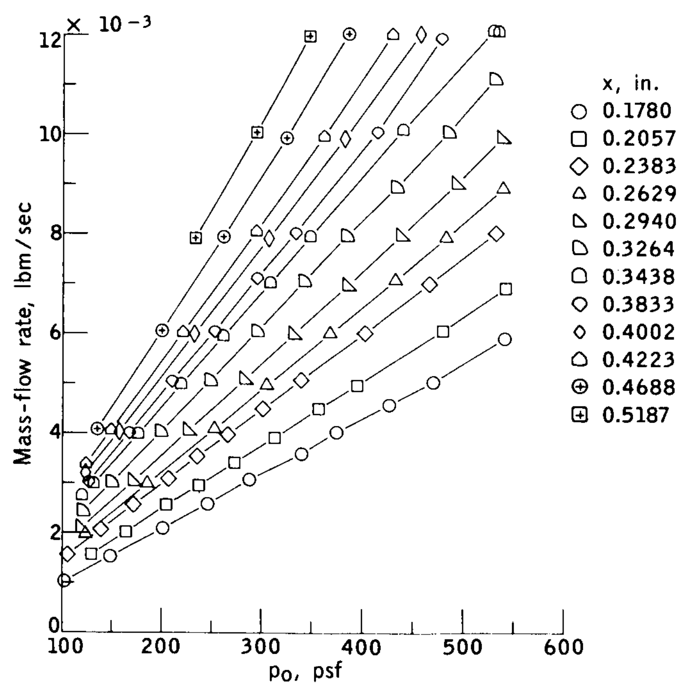

(c) Temperature, 75°F.

Figure 13. Mass-flow-rate data for 3/4-inch calibration valve.

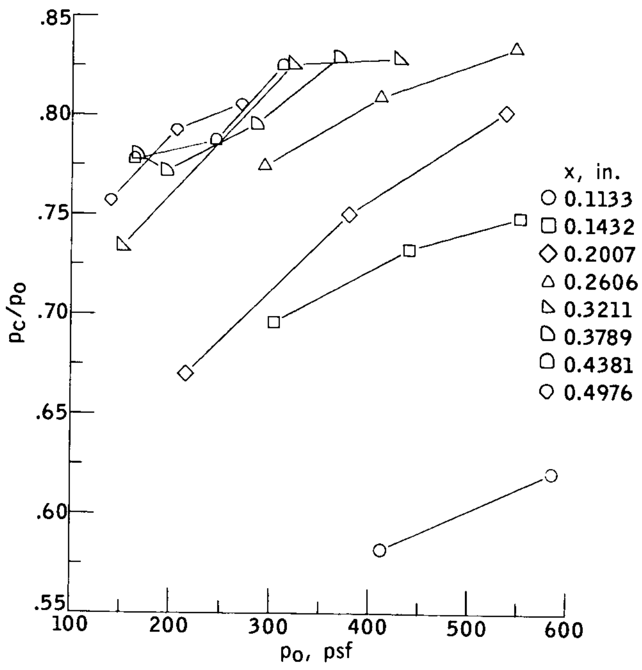

(a) Temperature, −30°F.

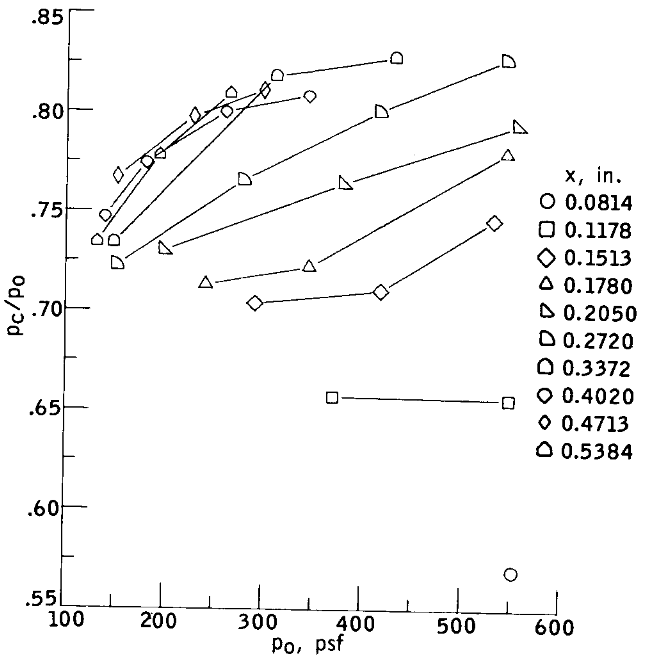

(b) Temperature, 10°F.

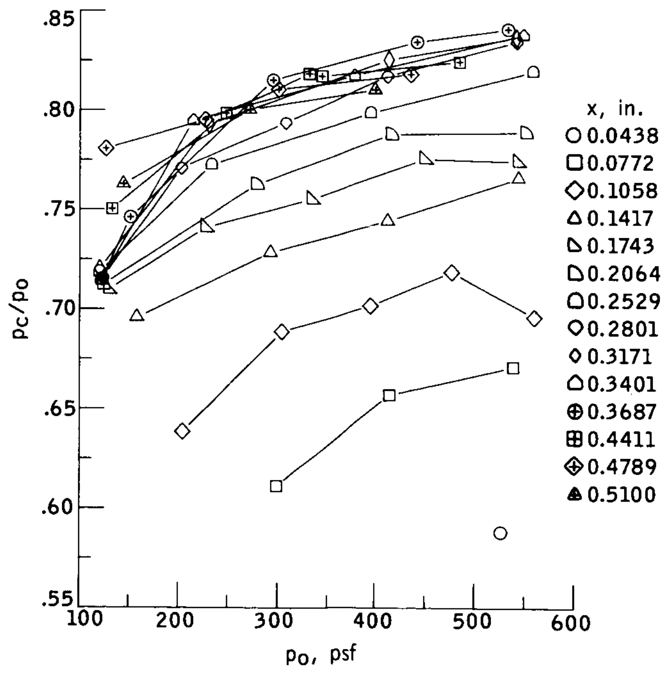

(c) Temperature, 75°F.

Figure 14. Choke pressure data for 5/8-inch calibration valve.

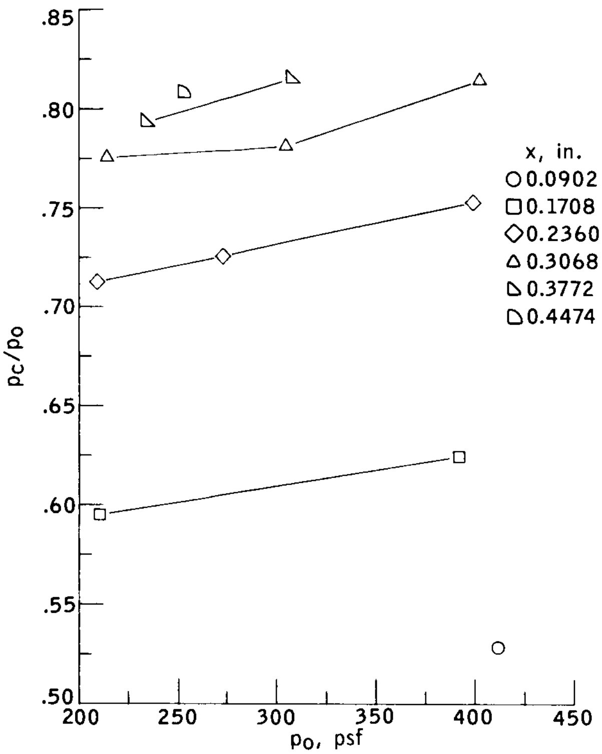

(a) Temperature, −30°F.

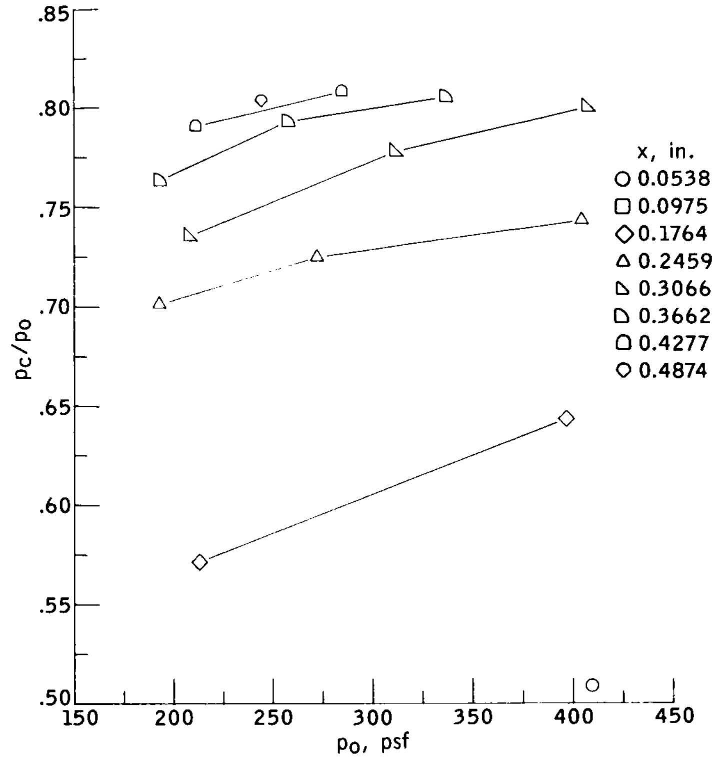

(b) Temperature, 10°F.

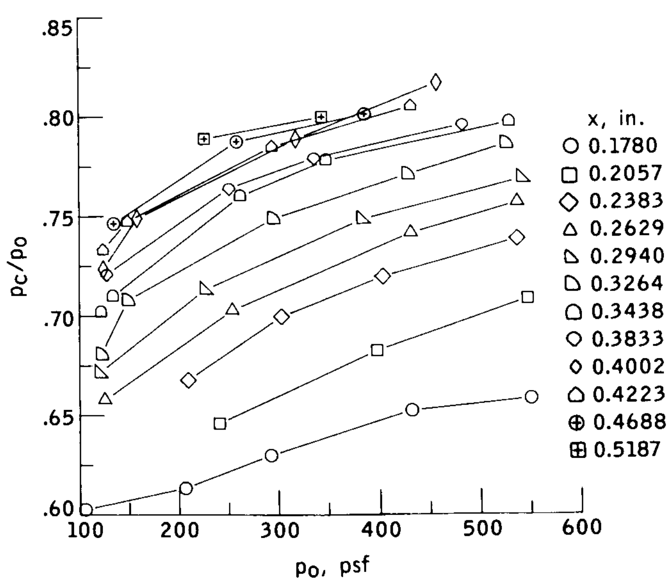

(c) Temperature, 75°F.

Figure 15. Choke pressure data for 3/4-inch calibration valve.

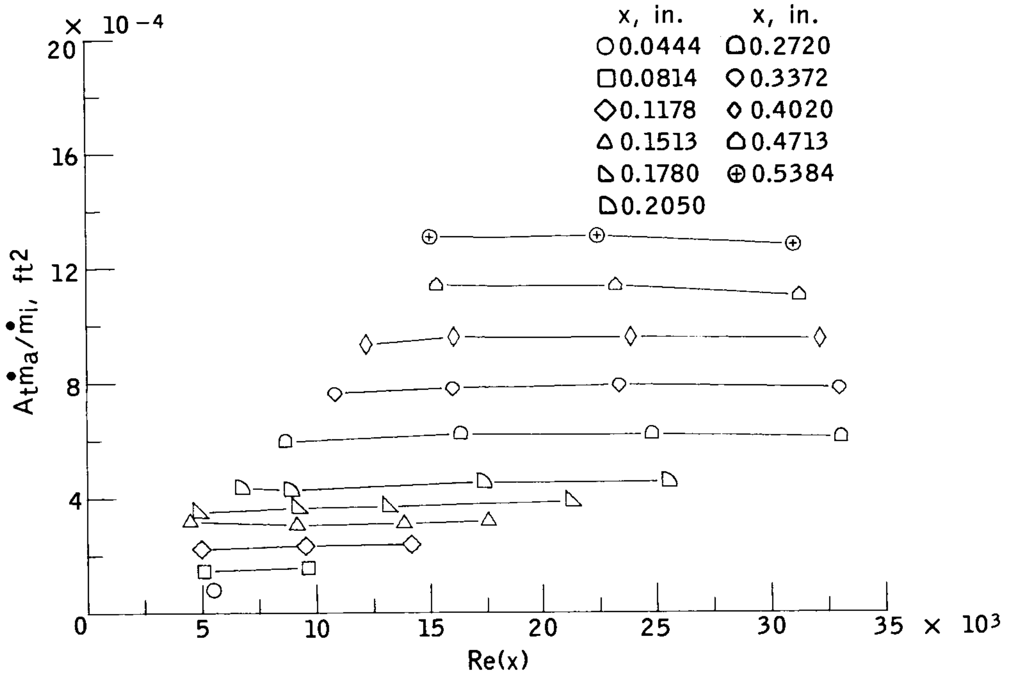

Figure 16. Mass-flow-rate ratio versus Reynolds number for 5/8-inch valve at 10°F.

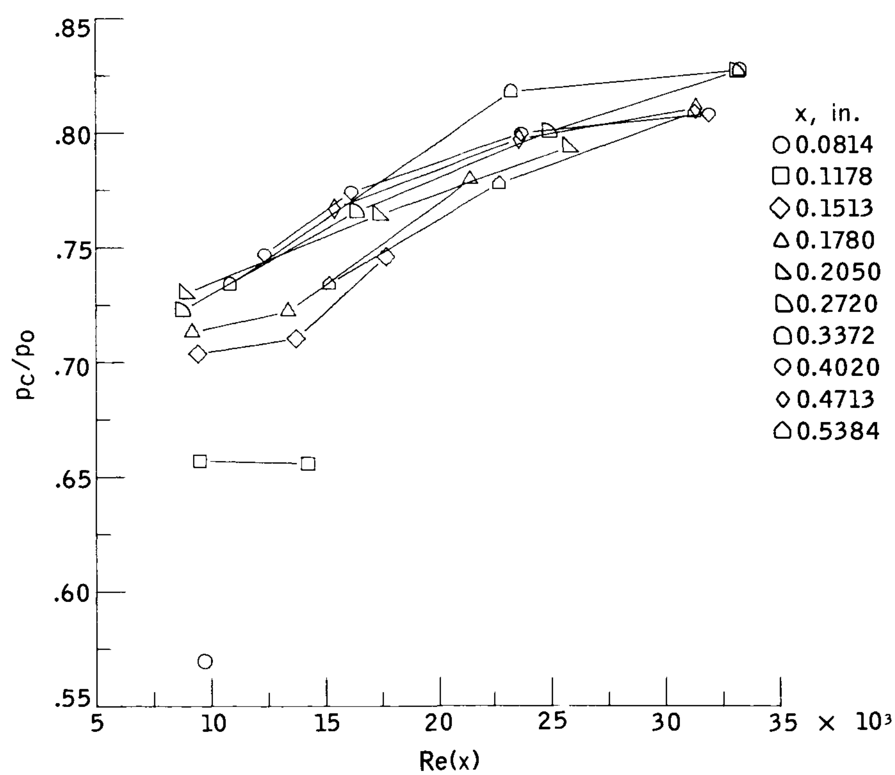

Figure 17. Pressure ratio versus Reynolds number for 5/8-inch valve at 10°F.

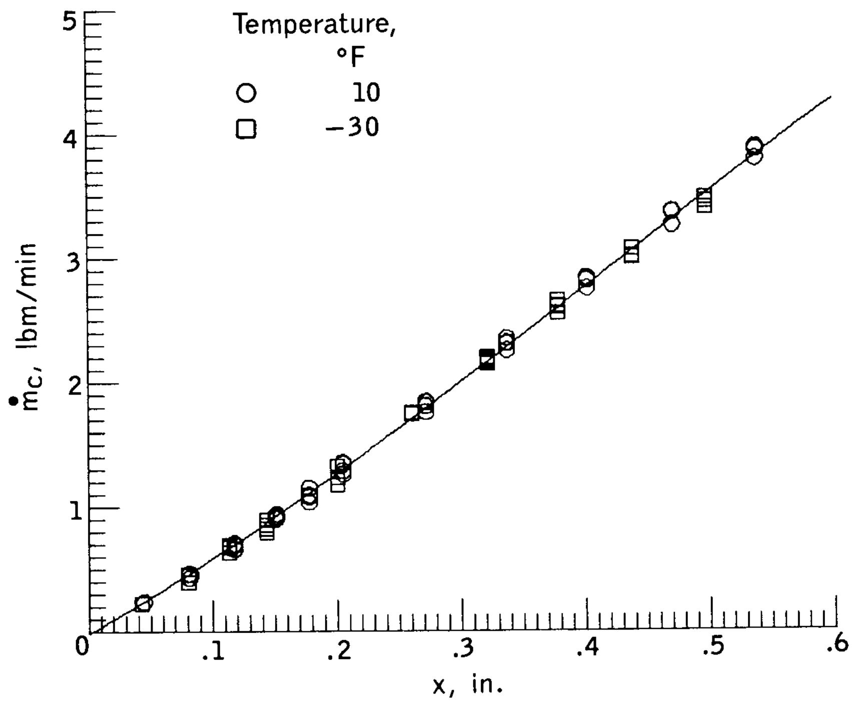

Figure 18. Correlation of corrected mass-flow rate for 5/8-inch valve at low temperature.

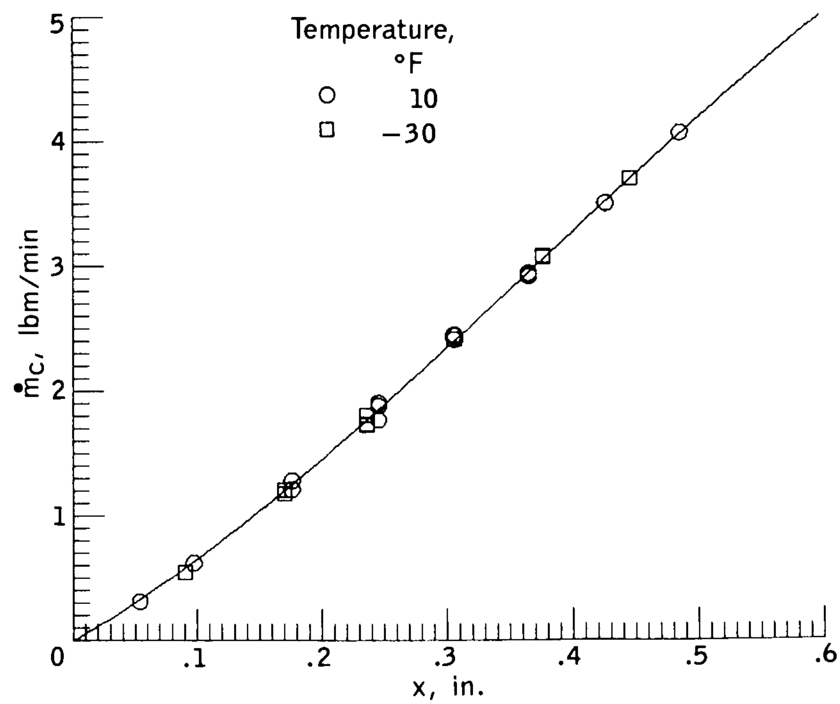

Figure 19. Correlation of corrected mass-flow rate for 3/4-inch valve at low temperature.

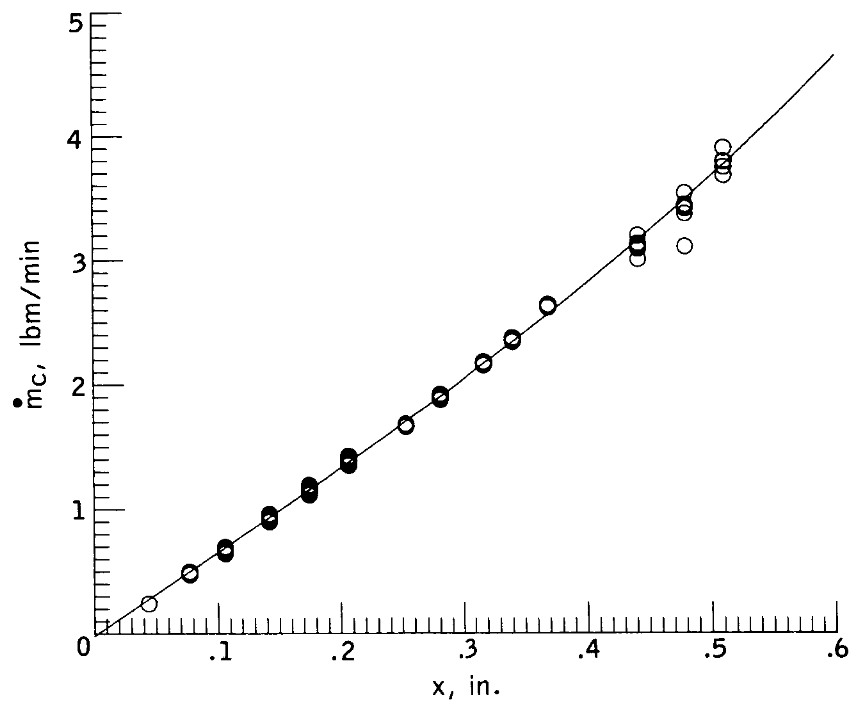

Figure 20. Correlation of corrected mass-flow rate for 5/8-inch valve at room temperature.

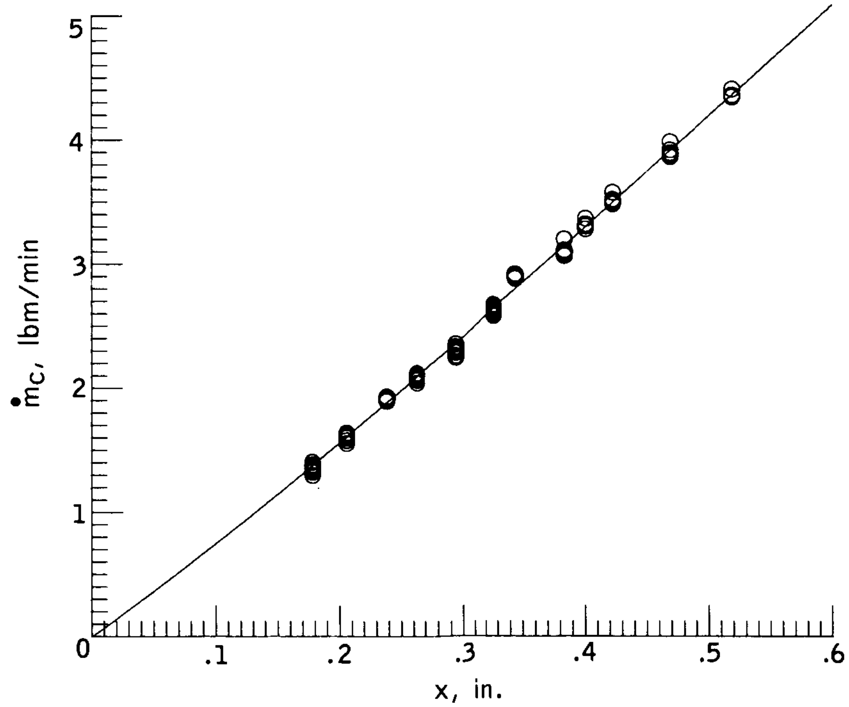

Figure 21. Correlation of corrected mass-flow rate for 3/4-inch valve at room temperature.

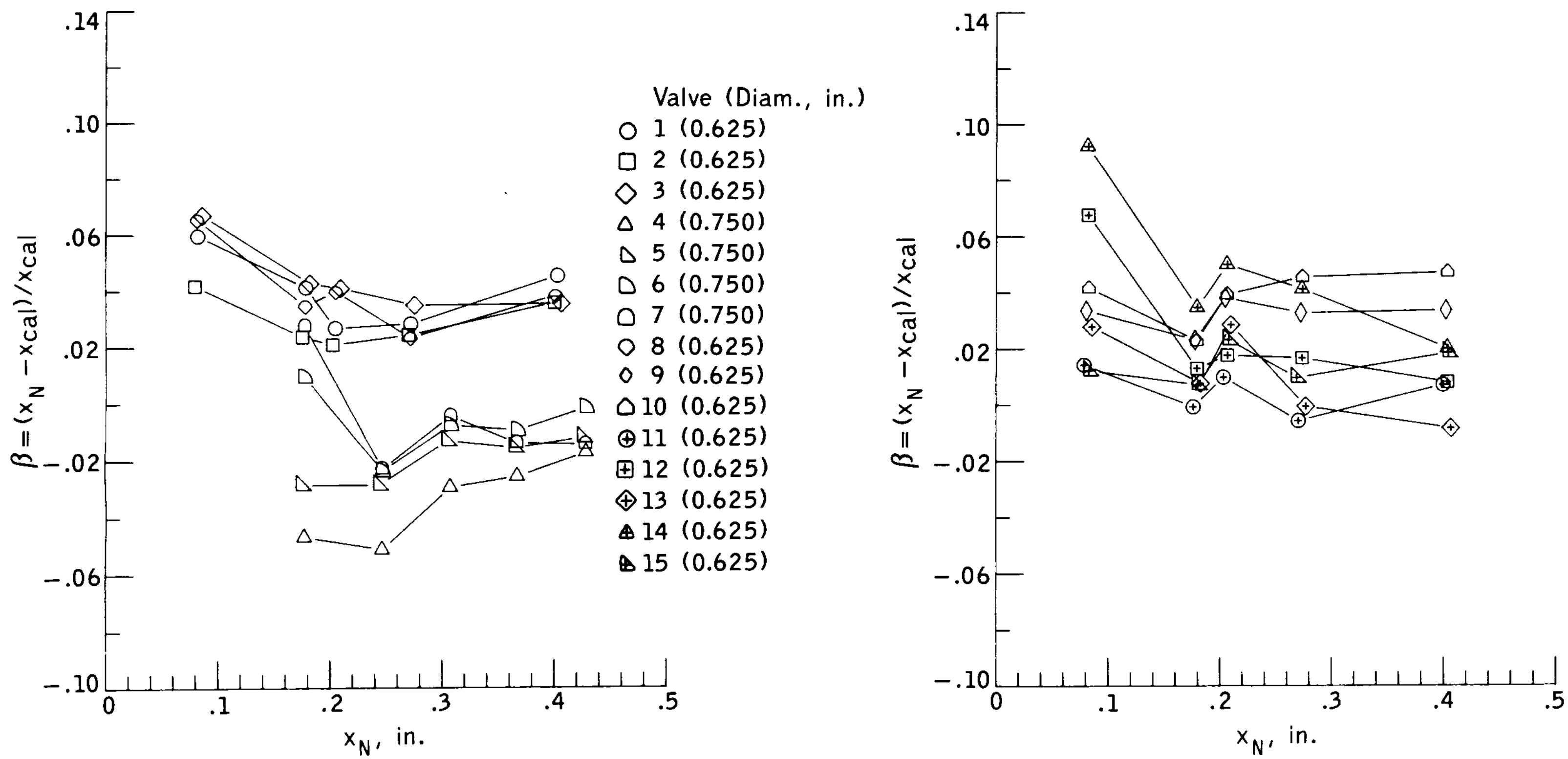

Figure 22. Flight valve correction factor β versus valve position x_N for chamber 1.

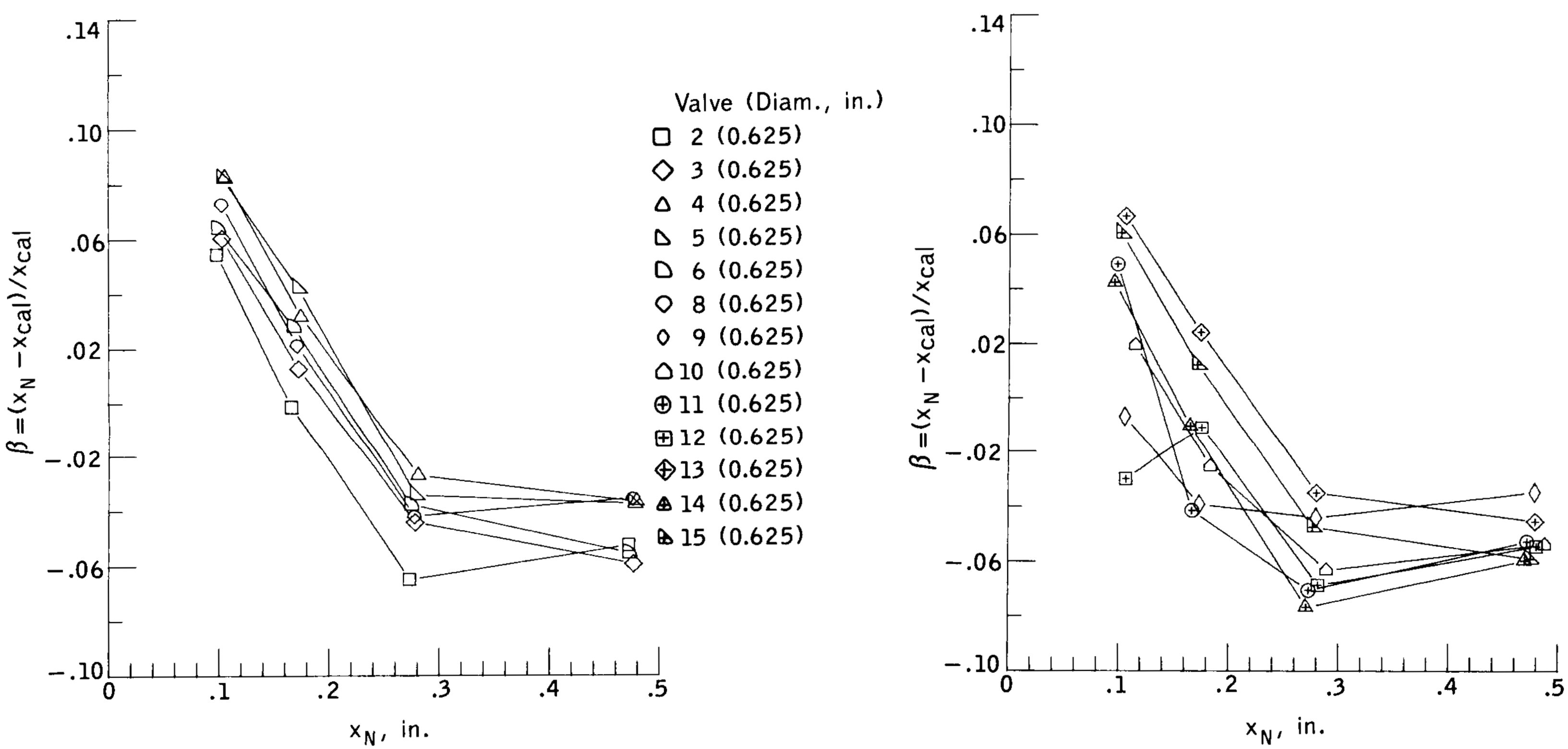

Figure 23. Flight valve correction factor β versus valve position x_N for chamber 3.

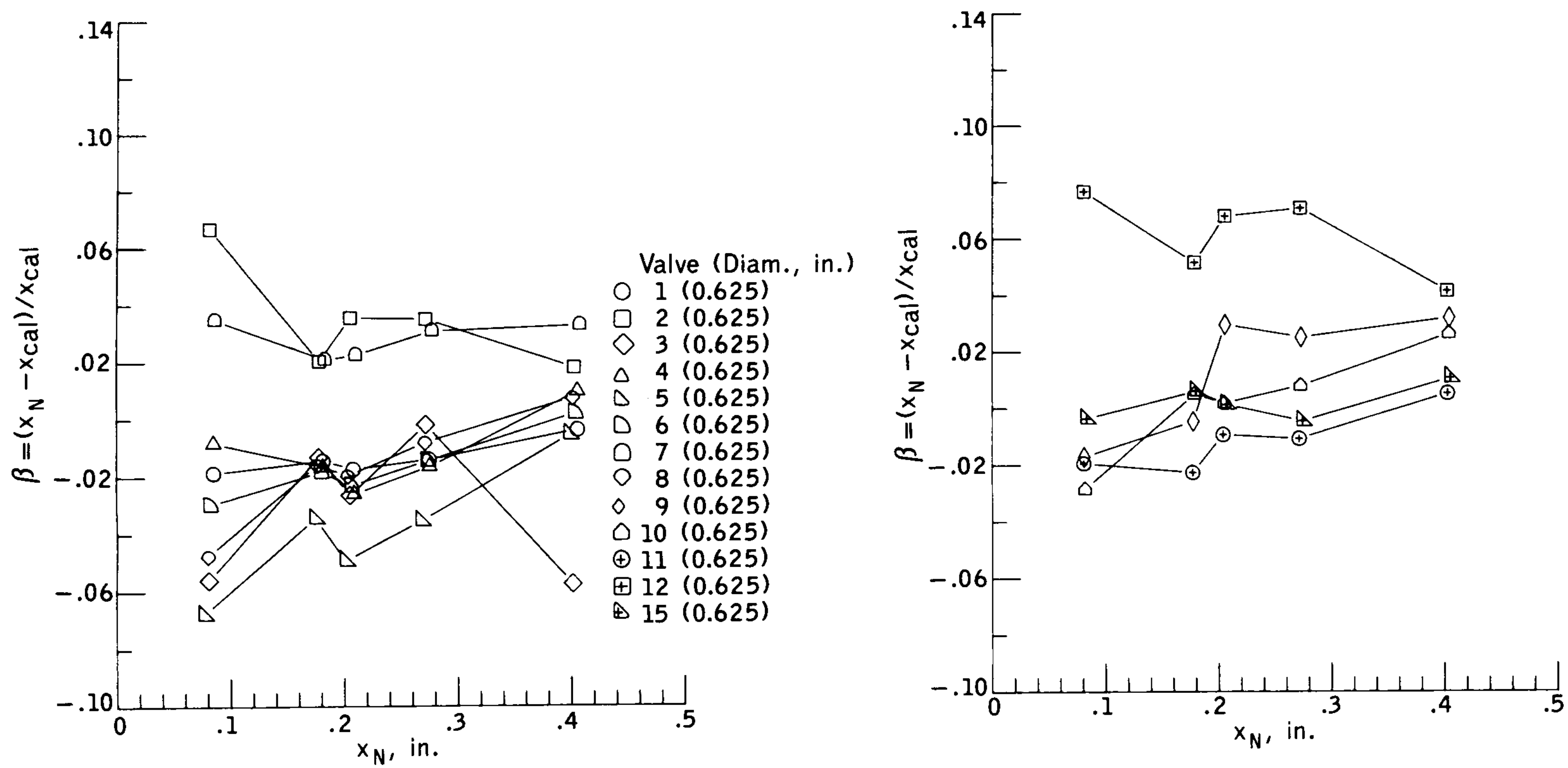

Figure 24. Flight valve correction factor β versus valve position x_N for chamber 5.

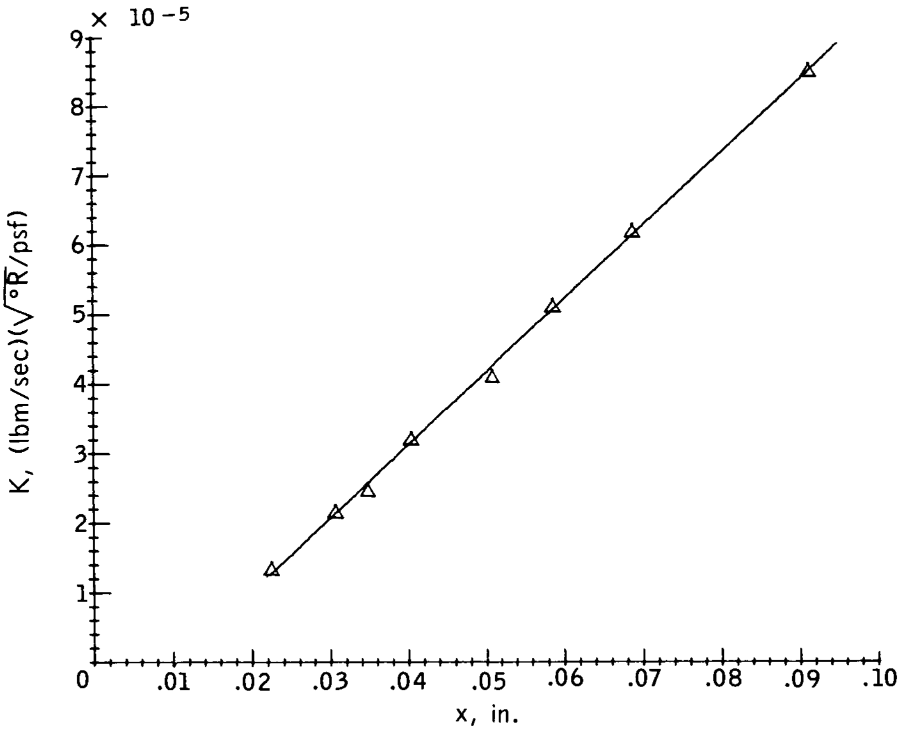

Figure 25. Purge flow correlation constant for subsonic flow in 5/8-inch valve.

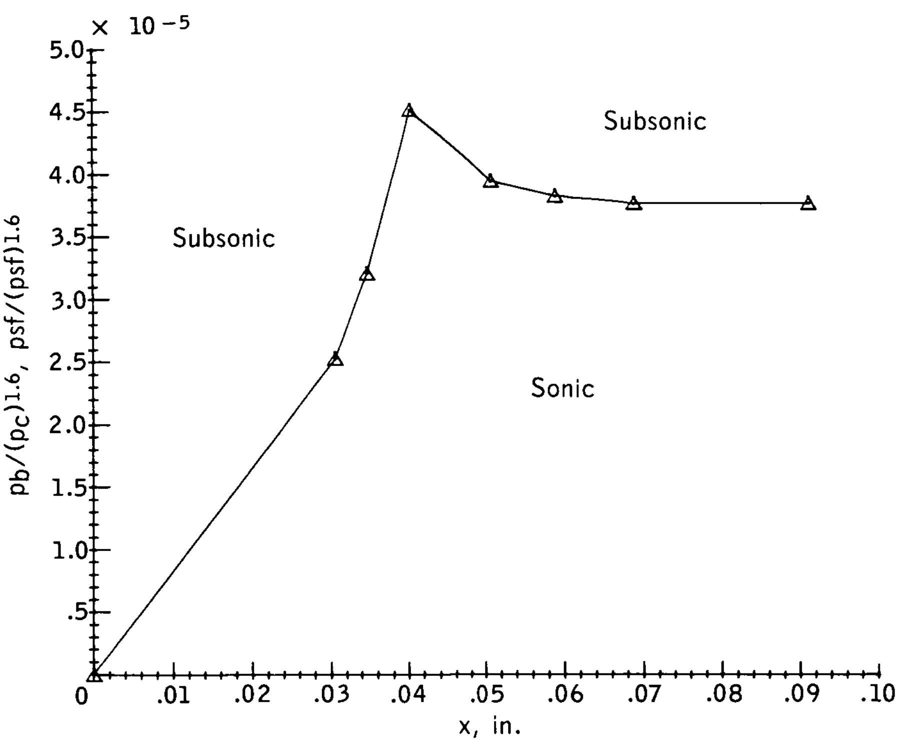

Figure 26. Pressure ratio threshold for sonic flow in 5/8-inch valve.

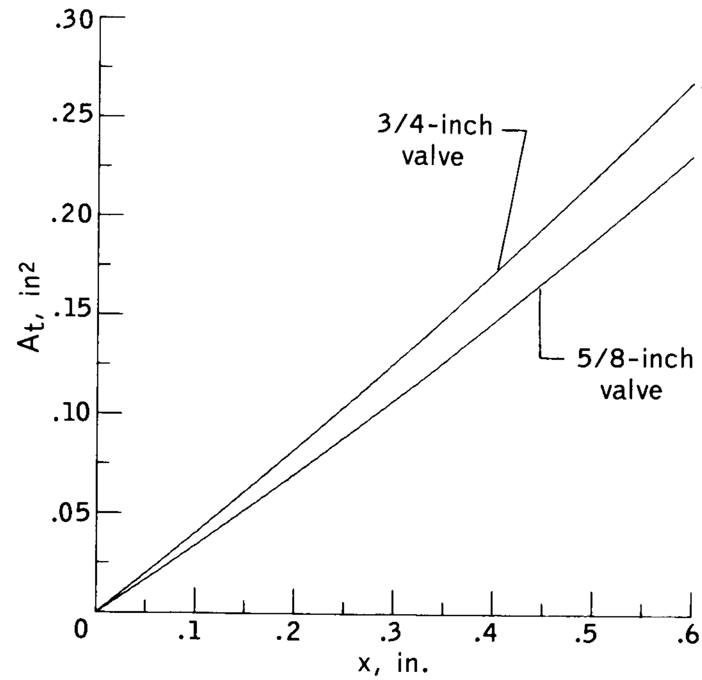

Figure 27. Nominal measured throat area versus needle position.

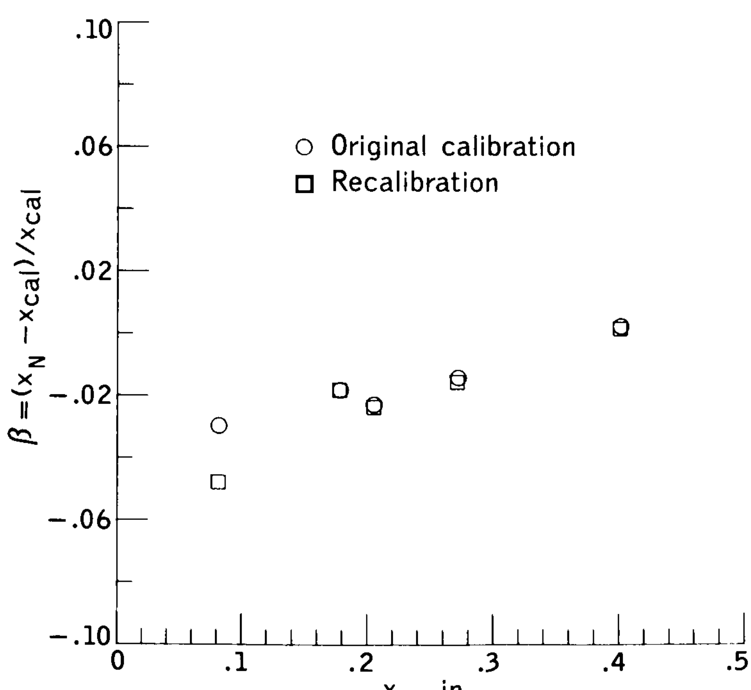

Figure 28. Repeatability of flight valve calibration β versus x_N for valve 6 of chamber 5.

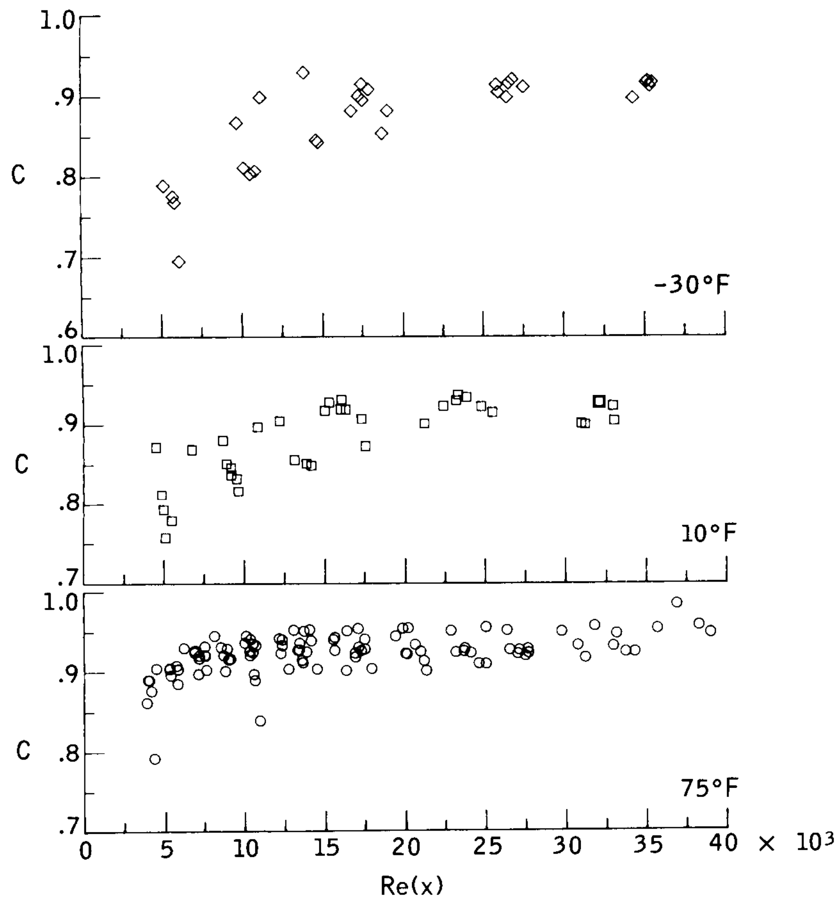

Figure 29. Discharge coefficient versus Reynolds number for 5/8-inch calibration valve.

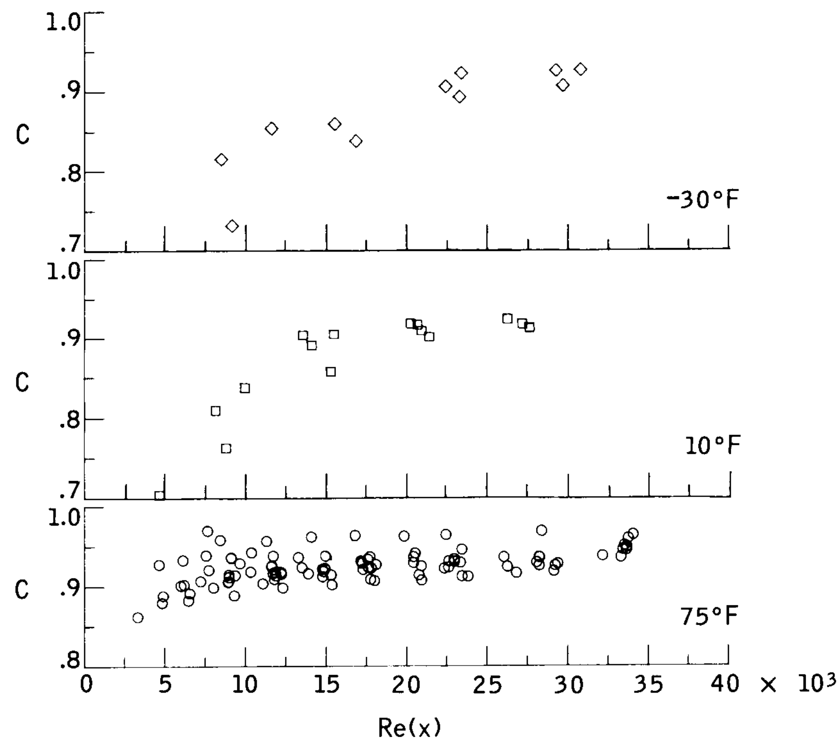

Figure 30. Discharge coefficient versus Reynolds number for 3/4-inch calibration valve.

1. Report No.	2. Government Accession No.	3. Recipient's Catalog No.
NASA TP-2423		

4. Title and Subtitle	5. Report Date
Calibration of Sonic Valves for the Laminar Flow Control, Leading-Edge Flight Test	May 1985
	6. Performing Organization Code 505-45-63-26
7. Author(s) Dennis H. Petley, William Alexander, Jr., Andrew S. Wright, Jr., and Maria Vallas	8. Performing Organization Report No. L-15893
9. Performing Organization Name and Address NASA Langley Research Center Hampton, VA 23665	10. Work Unit No.
	11. Contract or Grant No.
12. Sponsoring Agency Name and Address National Aeronautics and Space Administration Washington, DC 20546	13. Type of Report and Period Covered Technical Paper
	14. Sponsoring Agency Code

15. Supplementary Notes

16. Abstract

Sonic needle valves were calibrated to measure and control airflow in the suction system for the Leading-Edge Flight Test. The procedure and results for the calibration flow test of 41 flight valves are given. Mass-flow rates, which ranged from 0.001 to 0.012 lbm/sec, and maximum back pressures were measured for total temperatures from −30°F to 75°F and total pressures from 120 to 540 psf. Correlating equations were obtained for mass-flow rate as a function of total pressure, total temperature, and valve opening length. The most important aspect of flow measurement and control was found to be the measurement of valve opening length.

17. Key Words (Suggested by Authors(s))	18. Distribution Statement
Sonic valve Suction control Laminar flow control Mass-flow measurement Flow calibration Pressure ratio for choked flow Airflow Nitrogen flow	Unclassified—Unlimited Subject Category 02

19. Security Classif.(of this report)	20. Security Classif.(of this page)	21. No. of Pages	22. Price
Unclassified	Unclassified	51	A04

For sale by the National Technical Information Service, Springfield, Virginia 22161

NASA-Langley, 198

National Aeronautics and
Space Administration

Washington, D.C.
20546

Official Business
Penalty for Private Use, $300

THIRD-CLASS BULK RATE

Postage and Fees Paid
National Aeronautics and
Space Administration
NASA-451

U.S.MAIL

4 2 1U,A, 850425 S00161DS
DEPT OF THE AIR FORCE
ARNOLD ENG DEVELOPMENT CENTER(AFSC)
ATTN: LIBRARY/DOCUMENTS
ARNOLD AF STA TN 37389

NASA

POSTMASTER: If Undeliverable (Section 158 Postal Manual) Do Not Return